Design and Development of Turning Type Magnetorheological Finishing Process

A Dissertation Submitted
In Partial Fulfillment of the Requirements
for the Degree of

Master of Engineering

in

CAD/CAM & Robotics

by

Prince Garg

to the

MECHANICAL ENGINEERING DEPARTMENT

THAPAR UNIVERSITY, PATIALA

July, 2015

CERTIFICATE

I hereby declare that the thesis entitled "**Design and development of turning type magnetorheological finishing (MRF) process**" is an authentic record of my study carried out as requirements for the award of the degree of **Master of Engineering** in **CAD/CAM & Robotics** at **Thapar University, Patiala** under the supervision of **Dr. Anant Kumar Singh**, Assistant Professor, Mechanical Engineering Department, Thapar University, Patiala during July, 2015. The matter embodied in this report has not been submitted in partial or full to any other university or institute for the award of any degree.

Date: 13/07/2015

Prince Garg
Roll no. - 801381014

It is certified that the above statement made by the student is correct to the best of my/our knowledge and belief.

14/07/2015

Dr. Anant Kumar Singh
Assistant Professor
Mechanical Engineering Department
Thapar University, Patiala - 14700

Countersigned by

Dr. S. K Mohapatra
Sr. Professor & Head
Mechanical Engineering Department
Thapar University, Patiala - 147004

Dr. S.S Bhatia
Dean of Academic Affairs
Thapar University, Patiala - 147004

Acknowledgements

I am highly grateful to the authorities of Thapar University, Patiala for providing this opportunity to carry out the report work.

I would like to express a deep sense of gratitude and thank profusely to my thesis guides **Dr. Anant Kumar Singh** for their sincere & invaluable guidance and suggestions which inspired me to submit thesis report in the present form.

I would also like to thank all the faculty members of Mechanical engineering department for their intellectual support and unyielding encouragement.

I am deeply indebted to all my friends who helped me with their encouragement, ample morale support and valuable suggestions.

Finally, I would like to extend my gratitude to all those persons who directly or indirectly helped me in the process and contributed towards this phase of my report work.

Prince Garg

Abstract

A new precision finishing process for finishing of cylindrical external surfaces using turning type magnetorheological finishing tool has been developed. To fulfill the needs for finishing external cylindrical surfaces such as groove, taper, step surfaces and threads, a turning type magnetorheological finishing process has been developed. A newly developed turning type magnetorheological finishing process is used for finishing external cylindrical surfaces, as tool tip is able to reach deeper grooves. For this reason the turning type magnetorheological finishing process has been developed for further applications with the aim of achieving finishing in the external cylindrical workpiece surfaces.

At first simulation for turning type magnetorheological finishing tool were performed in MAXWELL ANSOFT V13 student version to study the magnetic flux density distribution at the tip of finishing tool. The second stage CAD model was designed for the turning type magnetorheological finishing tool to examine the shape and dimensions. With the designed parameters, a turning type magnetorheological finishing tool has been fabricated and attached at the selected Lathe machine.

To know the process capability of the developed finishing setup, the design of experiments was carried out with major selected process parameters such as working gap, magnetizing current and workpiece rotating speed. The experiments plan and analysis have been done by using software DESIGN EXPERT- 9. The experimental responses were measured in terms of percentage change in R_a values. The experiments have been performed on each specimen at 90 minute of finishing time. On the basic of experimental results, the optimum process parameters were predicted from the regression model for maximum percentage change in Ra value. The scanning electron microscopy has been also used to know the final finished surface quality. The newly developed turning type magnetorheological finishing process finds its broad function in automotive, machine tool manufacturing, valve and pipe manufacturing industries etc.

Content

List of Figures

List of Tables

Nomenclature

R_a	Average roughness value
R_z	Average space between the maximum peak and the lowly valley in each sample length
R_q	Root mean square value
Ra_i	Initial average roughness value
Ra_f	Final average roughness value
ΔR_a	Change in average roughness value
I	Electric current
N	Rotation speed of workpiece
Z	Working gap between the tool tip and the work surface

Greek Symbols

µ	Micro

Acronyms

ANOVA	Analysis of Variance
MRF	Magnetorheological Finishing
SEM	Scanning Electron Microscope
RTD	Real Temp Display
MR	Magnetorheological
MRP	Magnetorheological Polishing
2FI	Two Factor Interaction
S.D	Standard Deviation
C.V	Coefficient of Variance
C.I	Confidence Interval
VIF	Variance Inflection Factor

Chapter 1

Introduction

1.1 Introduction

The grinding, lapping and honing are used as traditional finishing processes. These finishing processes are less compatible regarding the size and shape of the material for finishing. The large amount of normal force is induced on the workpiece surfaces during the finishing operation that may results in different types of defects such as micro-crack, micro-cutting etc which decrease the material life as well as its strength. Lapping is carried out to finish flat surfaces, whereas honing is used to finish cylindrical internal surface. The poorer surface finish affects the fatigue life of the material (Bayoumi *et al*., 1995). During these finishing processes lesser control over the forces results in lesser control over the surface finish (Shaw, 1996).

1.2 Traditional process used for surface finishing

The different types of Traditional finishing techniques such as grinding, lapping and honing are available. These processes use abrasive type multipoint cutting tools, to perform various types of cutting as well as finishing operations. The force induced during these operations forms cracks on the surface of material (Hoshino *et al*., 2001). All these processes used in past to produce smooth surface at closer tolerances. The different type of traditional finishing processes is explained as following:

1.2.1 Grinding

Grinding is most broadly used finishing process among the various traditional finishing processes. During this process material removal takes place by the relative motion between the workpiece and abrasive wheel. When these abrasive particles come in contact with workpiece the machining is to be performed. It is used for fine finishing where accurate dimensions are needed. Each grain of the grinding wheel works as the single point cutting edge that performs machining during finishing.

1.2.2 Lapping

Lapping is mostly used for finishing of a flat workpiece surface. The main principle of lapping process is the abrasion action by the hard abrasive particles entrapped between the work materials.

1.2.3 Honing

Honing is mainly used for finishing of internal as well as external surfaces. In the honing, the honing tool is made up of abrasive particles is used for finishing. As the tool rotates into the internal surface of cylindrical workpiece, the finishing takes place.

1.3 Advanced finishing processes

Now a days for complex 3D shaped components with a nano level of surface finishing most in demands. The precise surface accuracy lies in the range of 10-100 nm, whereas for surface micro roughness is less than 10 nm RMS can be achieved with these processes (Zantye *et al*., 2004). These advance finishing processes are controllable processes whose forces can be easily controlled through external magnetic field for obtaining high product quality and also for polishing the materials (Jain *et al*., 2007; Zhong. 2008). The advanced finishing process as explained following:

1.3.1 Abrasive flow finishing

AFF process was originally recognized for deburring and finishing of the component (Jain, 2009). This process can finish in any medium i.e. air, liquid or fuel flow. AFM uses the abrasive particle together with the carrier for a finishing of the wear resistant material. The main components of this process are two perpendicularly opposed cylinders and extrudes abrasive medium between workpiece and tool as shown in Fig.1.1. Rheological property of fluid is responsible for change in abrasive action when it enters and pass from end to end the limiting passage (Rhoades, 1988, 1991).The viscosity of polymeric medium plays an significant character in finishing operation (Jha, 2006). The axial force component is accountable for the subtraction of chip, whereas radial force is responsible for the indentation of abrasive onto the workpiece. Parametric optimization is essential, for any type of manufacturing operations which were effort in case of AFF (Jain and Jain, 2000; Jain et al., 1999).

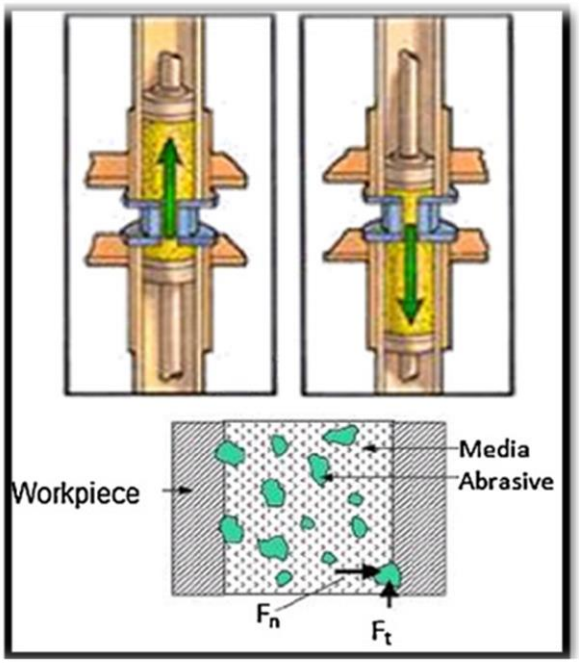

Figure 1.1: Schematic diagram of abrasive flow finishing process (Jain, 2009)

1.3.2 Magnetic abrasive finishing

For large dimension workpiece made up of hard to machine material nano level of surface finish is achieved by the magnetic abrasive finishing (MAF) process (Shinmura, 1987).

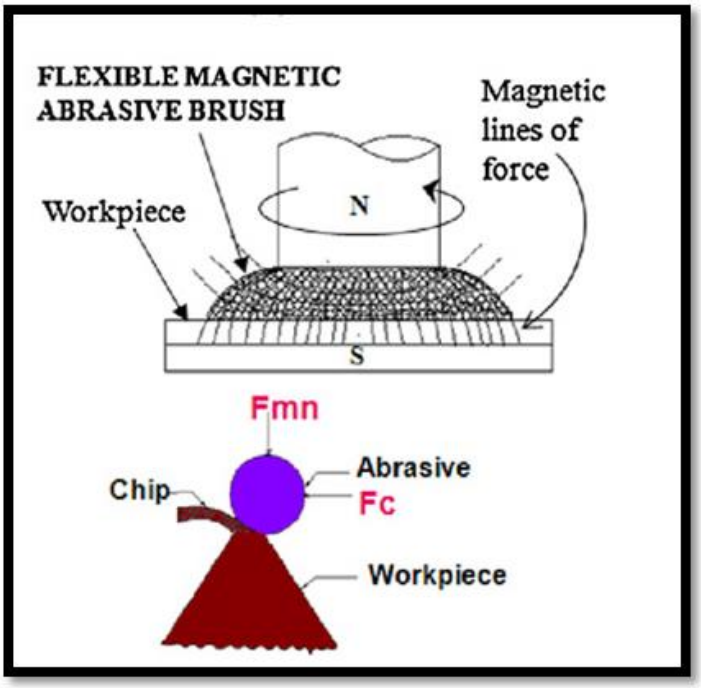

Figure 1.2: Schematic diagram of magnetic abrasive finishing process (Jain, 2009)

In MAF frequently ferromagnetic particles are sintered with fine abrasive such particles are called ferromagnetic abrasive particles. MAF schematic diagram is shown in Fig. 1.2 in MAF process the finishing deed is restricted by the applications of magnetic field crosswise the

working gap (Jain, 2009). The normal component force because of magnetic abrasive particles is responsible for the penetration of magnetic abrasive particles onto the workpiece. This machining action is restricted by controlling the magnetic field in the working space between the workpiece surface and the bottom face of the rotating electromagnet pole. Due to magnetic flux density the magnetic abrasive finishing is achieved and nano level of finishing is achieved on the work surface.

1.3.3 Magnetic float polishing

The MFP process is for cylindrical surfaces or for the 3D complex surfaces as well as the spherical surfaces as shown in Fig.1.3 below.

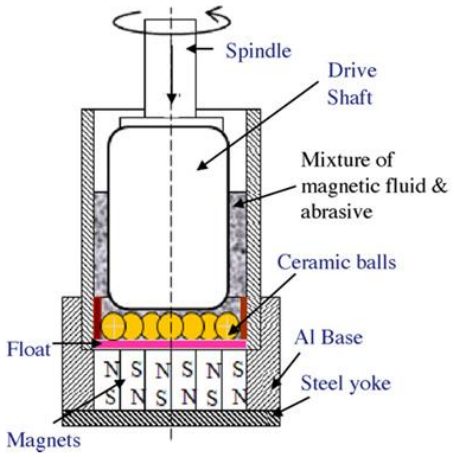

Figure 1.3: Schematic diagram of magnetic float polishing process (Jain, 2009)

Magnetic float polishing process is used for the accurate finishing of the ceramics balls and bearing rollers with the help of fine abrasive particles. The experimental setup and mechanism of magnetic float polishing process is shown in Fig. 1.3. it is carried out by the hydrodynamic actions of magnetic fluid and due to the use of magnetic field that rise abrasives and a non-magnetic float overhanging in it. The shaft is moved downhill to contact the ceramic balls and push them downward to gather the desired force level. Due to the influence of force and relative motion between the balls and abrasives, the balls are highly polished.

1.3.4 Magnetorheological finishing

The glass and high precession lenses are made of brittle material which cracks through machining action. To overcome these difficulties a technology has been developed known as magnetorheological finishing (MRF) as shown in Fig 1.3 (Kordonski, 1996). Magnetorheological fluid consists of a magnetic particle (such as carbonyl iron particles) and

abrasive particles diffuse in a non magnetic carrier such as mineral oil, silicone oil or water. The mechanism and experimental setup of magnetorheological finishing process is shown in Fig.1.4.

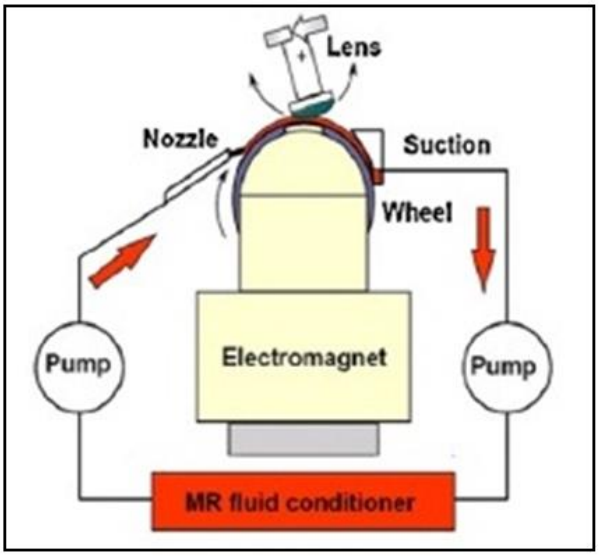

Figure 1.4: Experimental setup of magnetorheological finishing process (Jain, 2009)

Due to the result of outside magnetic field the CIPs becomes magnetize and shape a columnar structure.

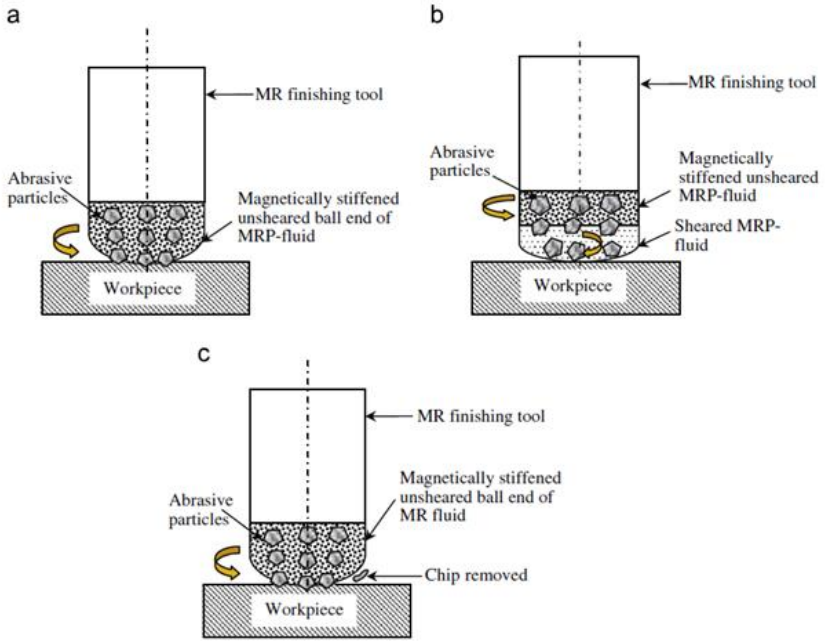

Figure 1.5: Finishing actions in the existence of magnetic field at the tip of the MRF tool (a) MR polishing fluid abrasive grains immediately reaching the irregularity peak (b) abrasive grains bit by bit progressing over irregularities in lack of sufficient bonding forces c) abrasive grains takes a minute scratch on irregularity mountain in the existence of sufficient bonding strength (Singh et. al. 2011).

Finishing stroke in the occurrence of magnetic field to the tip of the MR finishing tool as shown in Fig 1.5.(a) shows how abrasive grains in the MR polishing fluid reaches the roughness of the workpiece (b)how bonding force is responsible for finishing (c) abrasive grains remove the roughness peak in the form of chip. Bonding force is responsible for the finishing that is restricted by controlling the magnetic field intensity. As the magnetic lines are activated the MR fluid is stiffened at the tool tip and form a ball end shape having surface contact with tool tip and the work surface.MRF tool rotate and the workpiece reciprocates during finishing action.

1.3.5 Magnetorheological abrasive flow finishing (MRAFF)

MRAFF method consisted of CIPs particles, silicon carbide abrasive particles along with the base medium such as mineral oil, silicone oil or water. As the magnetic field amplify, the CIP particles forms a chain like structure over abrasive particles for nano finishing.

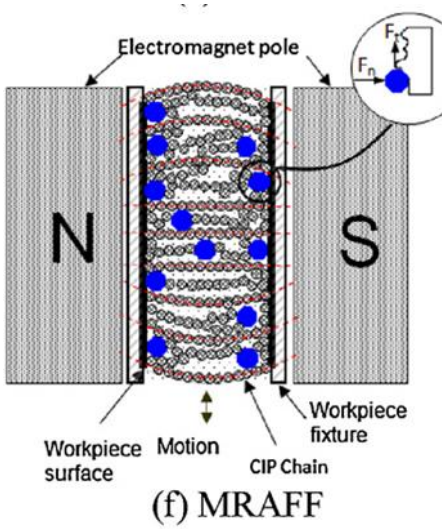

Figure 1.6: Mechanism of magnetorheological abrasive flow finishing process (Jain,2009)

As the magnetic flux density increases the CIP particles holds abrasives particles bonding strength depends upon the magnetic field that affects the material cut off at the mountain of workpiece surface. Mechanism of MAFF process is shown in Fig 1.6. The MRAFF process is mainly used for the finishing of 3D complex internal and external geometry, cylindrical internal and external surfaces, optical flats, spheres etc. Development of MAFF method is exposed in Fig.1.7.

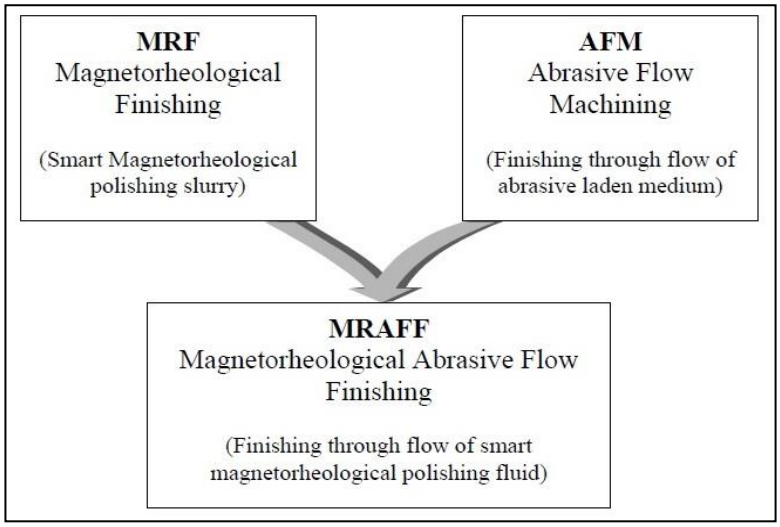

Figure 1.7: Development of magnetorheological abrasive flow finishing method (Jha and Jain, 2004)

The abrasives flow over workpiece in the deficiency of outer magnetic as well as finishing action at a particular profile when magnetic field is applied as shown in Fig 1.8.

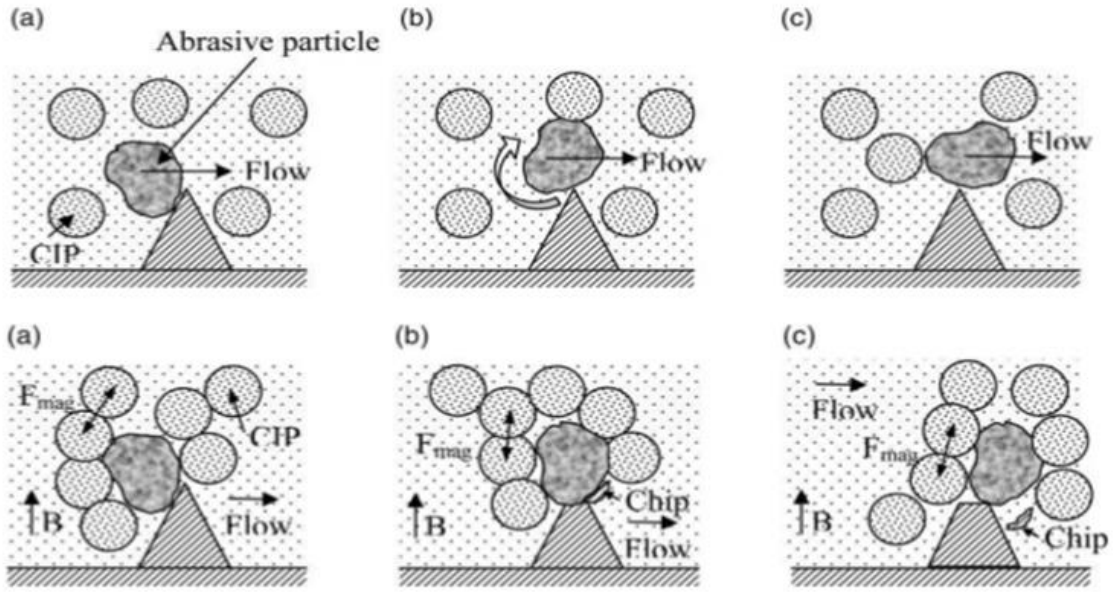

Figure 1.8: Finishing action at peaks in existence of exterior magnetic field, a) Abrasive grain beside by CIP chains reaching irregular surface; b) Abrasive grain obtains a minute shear of irregular surface in occurrence of bonding strength; c) Abrasive grain passage the roughness irregularities after removing a μchip through abrasive action(Jha and Jain, 2004).

1.3.6 Magnetorheological jet finishing

It is newly developed finishing process. This process is also known as modification of MRF

process in this MR fluid mixed with magnetic abrasive that is jetted into the work material in magnetized form when it flow through the nozzle. As the particles are highly magnetized when it passes through the internal surface of the workpiece, it becomes preciously finished. The jet snapshot image of magnetic abrasive jet finishing is as shown in Fig.1.9 when the magnetic field is off; the jet MR fluid jet passes through nozzle losses its coherence due to its high viscosity. When magnetic field is on the stable jet of MR fluid passes through the nozzle with low viscosity and high velocity jet as shown in Fig.1.9 below.

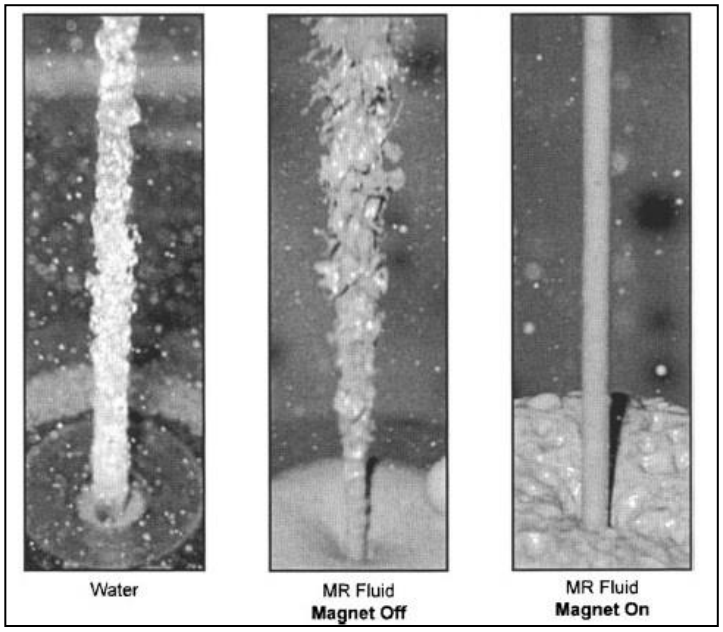

Figure 1.9: Jet snapshot image (velocity- 30 m/s, nozzle diameter- 2 mm) (Kordonski *et al*., 2006)

1.4 Mechanism of material removal in finishing

As the abrasive in contact with the work surface that perform the machining during finishing. The peaks at the work surface remove slowly and critical surface finish is obtain by the given conditions as shown in Fig 1.10 cross section along A-A.

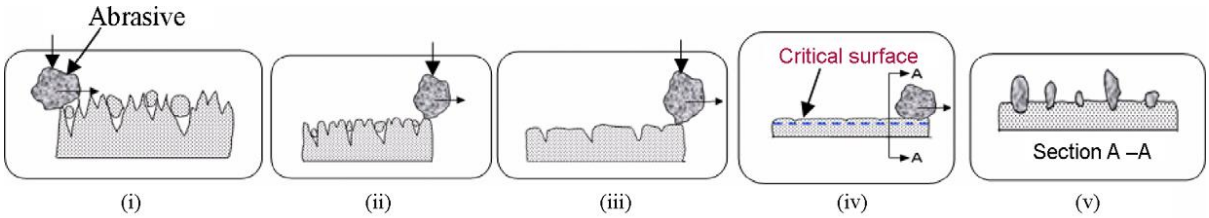

Figure 1.10: Steps (i) – iii)) material cut off at workpiece surface, iv) significant surface finish attain for finishing situation, (v) Cross-section beside A-A(Jain,2009).

1.5 Advantage of advanced finishing processes

- Closer tolerances can be achieved.
- Capable to accessing hard to reach areas.
- These processes are controllable processes.
- Increase the life of the work material.
- Better sealing capabilities.
- Decreasing the wear and friction losses.
- Used for finishing of internal and external surfaces.
- Reduces the surface defects (such micro cracks, cavity etc.)

1.6 Application of advanced finishing processes

The advanced finishing processes have its wide applications in finishing of automotive parts such as bore of an internal combustion engine, connecting rod, cam shaft lobes, bearing race, fuel injector component etc. medical instrument, electronic component, finishing of dies, turbine component aerospace, automotive and machine tool manufacturing**,** packing seal manufacturing industries, valve and pipe manufacturing industries etc.

Chapter 2

Literature Review

2.1 Literature review

In this chapter literature review of various authors in the field of advanced nano finishing processes (for ferromagnetic and non ferromagnetic workpiece) and their observations are drawn in brief from the paper and are represented for better understanding.

Cheng *et al.*, (2008) worked on MR fluid for finishing of K9 glass mirror by wheel shaped polishing tool .(usually a mixture of 57.34% silicon oil ,33.84% carbonyl iron powder, 6% cerium agent and 2.82% stabilizing agent). The two sets are conducted for experimental studies (with/without abrasive particles). With viscosity- 8.9 Pa, voltage- 2V, time- 20 min the surface roughness decreases to 0.47 nm.

Das *et al.*, (2008) reported for finishing of stainless steel workpiece through magnetorheological abrasive flow finishing method the effect of number of cycles on the surface finish . The constituent of 20% SiC abrasive powder, 20% CIPs with 60% visco plastic base medium used for finishing done by MR fluid. For both experimental and theoretical cases the results concluded that the value of surface finish increases, through the increase in the number of cycles.

Jain, (2008) reviewed for making a precise finishing in the level of nanometer the performance of different abrasive flow finishing processes. Different shapes of work material such as spherical, complex, flat and cylindrical depending upon the type of finishing required is reviewed by author for different advanced finishing processes can be used for finishing.

Jain, (2009) studied the nano finishing method through outside forces and different types of finishing processes such as abrasive based advances micro and nano finishing processes. Work material and finishing condition are main criteria for selecting various finishing processes. The author also summarizes the various finishing processes.

Jha and Jain, (2006) calculated for finishing of stainless steel the effect of different grades of CIPs particles (CS and HS) on the surface finish by using magnetorheological abrasive flow finishing process. Usually a mixture of 20% CIPs, 20% SiC abrasive powder and 60% visco plastic base medium MR fluid is used for finishing. The Table No 2.1 shows the results

concluded that higher improvement in surface roughness between 0.32-0.09 µm was made by using CIPs (CS) with SiC-800 mesh size.

Table 2.1: Surface roughness results (Jha and Jain, 2006)

Expt. No.	CIP dia. (D_{CIP}) (µm)	SiC dia. (D_{SiC}) (µm)	D_{CIP}/D_{SiC}	Initial Ra (µm)	Final Ra (µm)	ΔRa^a (µm)	%ΔRa
1.	18.0 (CS)	19.00	0.95	0.32	0.09	-0.23	-17.87
2.	18.0 (CS)	12.67	1.42	0.28	0.17	-0.11	-39.28
3.	18.0 (CS)	7.50	2.40	0.31	0.23	-0.08	-25.80
4.	3.5 (HS)	19.00	0.18	0.26	0.23	-0.03	-11.54
5.	3.5 (HS)	12.67	0.28	0.28	0.24	-0.04	-14.28
6.	3.5 (HS)	7.50	0.47	0.25	0.24	-0.01	-4.00

Das et al. (2012) study the result of extrusion pressure and working cycles at vary in surface roughness ΔRa in order to compare the performance of R-MRAFF with MRAFF. CIPs, SiC abrasive particles along with visco plastic medium are used for finishing. Stainless steel, brass and EN-8 work materials is used for the preliminary experiment. The result concluded that the least improvement in surface finish was observed in case of EN-8 and highest improvement in surface finish was observed in case of brass. ANOVA method was used for the experimental analysis. The process parameters are Ratio of CIP/SiC, number of finishing cycles, pressure by extrusion and rotational speed. The result

on surface irregularities. Surface roughness reduces with the rise in the quantity of SiC particles, whereas MRR increases.

Shankar *et al*., (2010) performed theoretical and experiment investigation on three types of work material namely Al alloy, Al alloy/SiC MMC with 10% SiC and Al alloy/SiC MMC with 15% SiC by R-AFF process for comparing the performance of ΔRa and MR at different rotational. The results as shown below concluded that the R-AFF yields better hardness and higher MRR as compared to the AFF in case of Al alloy/SiC (10%) MMC.

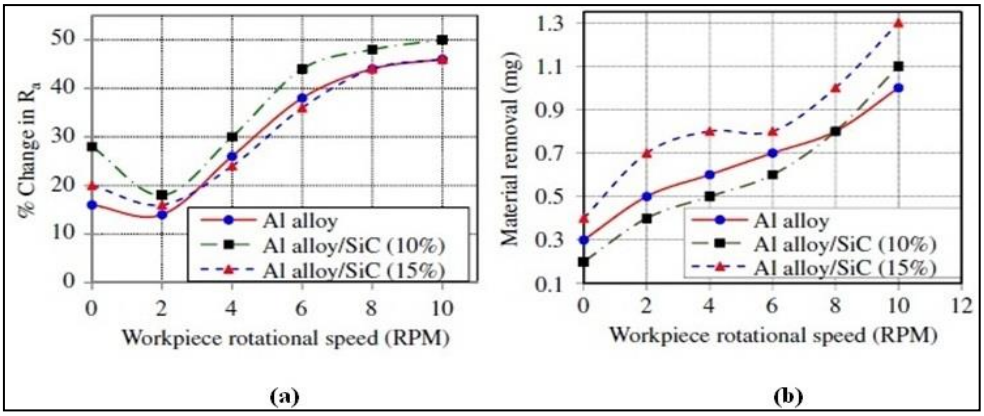

Figure2.2: Effect of workpiece on rotational speed on (a) Ra (b) MR for the three workspaces (speed-550 RPM, pressure- 6.25 MPa, M-10%) in AFF (RPM- 0) and in R-AFF (Shankar et al., 2010)

Singh *et al.* (2012) performed experiment with different projections (such as flat, 30^o, 45^o and 50^o curve surface) for finishing of ferromagnetic magnetic material by using ball end magnetorheological finishing tool as illustrated in Fig 2.2. The finishing was carried out with MR fluid (usually a mixture of 20% CIPs, 20% SiC abrasive powder and 60% visco plastic base medium.

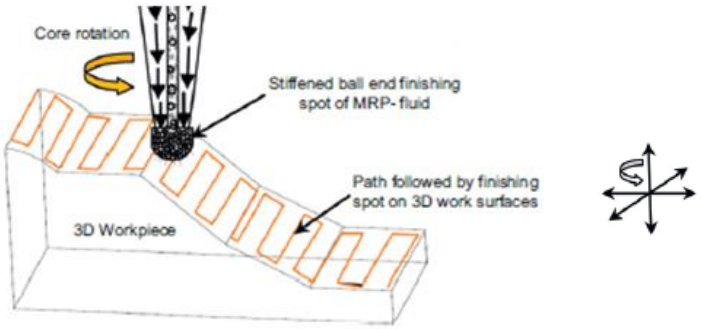

Figure 2.3: Schematic of a ball end MR finishing process of the typical 3D workpiece surfaces (Singh et al., 2012)

The results concluded that the surface roughness of flat, 30^o, 45^o and 50^o curve surface

reduces to 18.7 nm, 30.4 nm, 71.0 nm and 123.7 nm.

Singh *et al.*, (2013) evaluated the effect of working gap in the theoretical and experimental investigation on MRR by using ball-end MR finishing tool for finishing ferromagnetic material. Normal forces are calculated by using mathematical for calculating the normal force. The finishing was carried out with MR fluid (usually a mixture of 20% CIPs, 20% SiC

abrasive powder and 60% visco plastic base medium. The results concluded that with 0.66mm working gap the surface roughness decrease to 0.028 µm as illustrated in Fig 2.3.

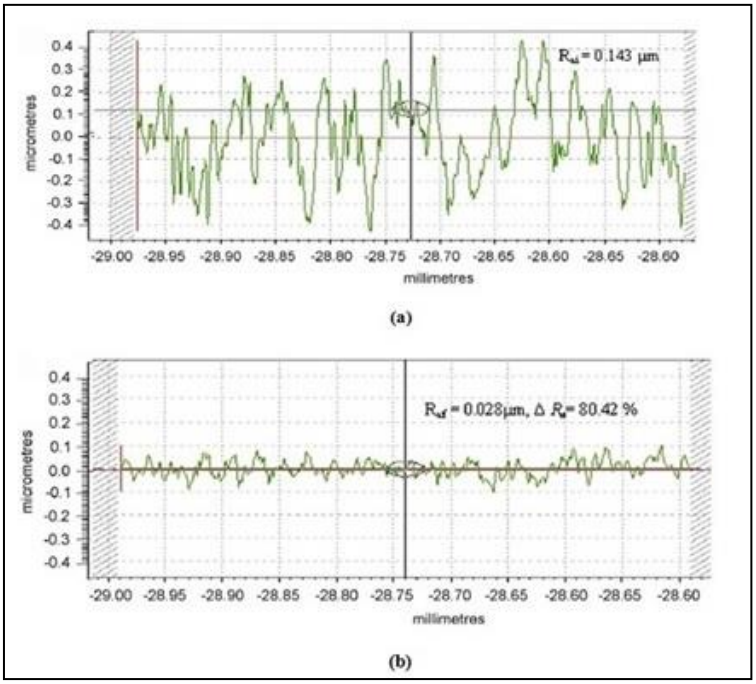

Figure 2.4: Surface roughness profile (a) Initial (b) After BEMRF at working gap 0.66 mm with Fn- 16.35 N (Singh *et al*., 2013)

Wang and Hu, (2005) The experimentation was carried out with 4 different types of abrasive particle were TiC/Fe (7% TiC), Al_2O_3/Fe (20% Al_2O_3), TiC/Fe (35% TiC), TiC/Fe (20% TiC) with a finishing fluid (stearinic acid and transformer oil). compare the performance of surface roughness and MRR with finishing time by using a magnetic assisted finishing process for finishing of Ly12 aluminum alloy, 316L stainless steel and H62 brass. The outcome accomplished the surface irregularities minimize with increase in finishing time where as the, MRR increases with increases in finishing time.

Sidpara and Jain, (2011) compare the performance of forces by using magnetorheological fluid based finishing process for finishing of single crystal silicon between the working gap and CIPs concentration. The authors used MR fluid (a mixture of CIPs, abrasive particle and glycerol). From the performance, it was concluded that the normal as well as tangential forces increase with enlarge in CIPs concentration and reduces with enlarge in working gap.

Yamaguchi and Shinmura, (2004) studied for finishing of alumina ceramic tube they performed experiment on the magnetic assisted finishing process. The experimentation was

performed by using diamond abrasive (0-1, 2-4, 4-8 and 8-12 µm) ,different iron particle (150, 330 and 510 µm) and lubricant (0.1, 0.2, 0.25, 0.3 and 0.35 ml). The results concluded that with the use of diamond abrasive (0-1 µm) , iron particle (330 µm) and lubricant (30 ml), the surface roughness reduces to 0.02 µm.

Singh *et al*., (2004) evaluated different working parameters to determine the effect of process variable on the surface finish by using a mixture of 25% SiC and 75% iron by magnetic abrasive process. The optimum parameters for obtain surface roughness are voltage-11.5 V, working gap-1.25 mm, speed-180 RPM as shown in Fig 2.4.

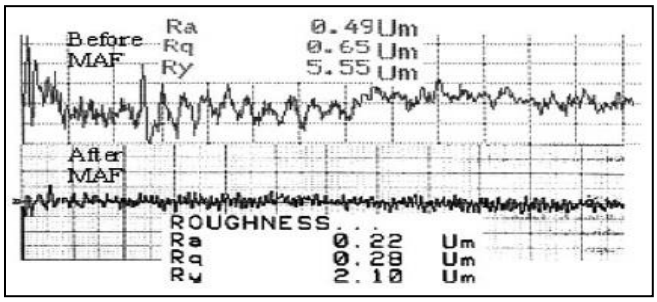

Figure 2.5: Surface roughness values before and after finishing (Singh *et al*., 2004)

Yin and Shinmura. (2004) compare the performance of surface roughness and deburring on three different substrates by using vibration-assisted magnetic finishing process. The finishing was carried out with process magnetic alumina, iron particles and straight oil type grinding fluid on stainless steel (SU304), magnesium alloy (AZ31B) and brass (C2680). The results concluded that the surface roughness and deburring was found to better in magnesium alloy (AZ31B) as compared to stainless steel (SU304) and brass (C2680).

Jha et al. (2007) performed their experiment to learning the result of extrusion pressure and amount of finishing cycles while finishing stainless steel work material on magnetorheological abrasive flow finishing method. The finishing was carried out with the help of (20% CIPs, 20% SiC abrasive particles and 60% visco plastic base medium. The result concluded that through the raise in amount of finishing cycle, extrusion pressure up to 3.75 MPa, the value of surface irregularity improves.

Das et al. (2010) worked on rotational magnetorheological abrasive flow finishing method for finishing of stainless steel work material. The finishing was carried out with the help of MR polishing (usually contains 26.6% Fe powder, 13.4% SiC abrasive through base medium). The effect of RPM of magnet, abrasive particle size and finishing time on the

surface roughness are measured with preliminary experimentation along with design of experiment and response surface regression analysis. The results concluded that with the increase finishing time (1600 sec) and in RPM (up to 150) the surface roughness founds to be better, whereas the surface roughness founds to be better with the decrease in abrasive particle size (150),.

Judal et al. (2013) developed a new vibration assisted magnetic abrasive finishing process for finishing of alumiuium workpiece. Steel grit and Al_2O_3 abrasive are used for finishing the aluminum workpiece. The effect of different process parameters such as, magnetic flux density as well as volume of abrasive particles, revolving speed, and frequency on material removal rate was studied. The result concluded that the surface roughness value Ra reduces to 0.18 µm, and with the increase in rotation speed and magnetic flux density and frequency of the vibration, that increasing the material removal rate.

Hong et al. (2012) performed their experiment on MR polishing for finishing of alumina reinforced zircon ceramics (3YTZP/Al_2O_3-20%). The finishing was carried out with MR fluid (50% CIPs, abrasive diamond particles and DI water). The process parameters in this experiment are (speed- 200 and 300 RPM, magnetic field- 3.8, 4.7, 5.5 and 6.1KA/m, Time- 10, 20, 40 and 60 min). The optimum parameter with results concluded that with 300 RPM, magnetic field- 3.8 KA/m and electric current- 0.5 Amp the surface roughness decreases from 0.272 µm to 1.960 nm.

Cheng et al. (2010) developed a dual axis MRF tool with internal magnet for finishing of BK7 mirror. The finishing was carried out with the help of MR fluid (includes 10% CeO_2 abrasive particles). The material removal is calculated by mathematical modelling by mathematical calculations. The process parameters were (polishing time- 1 min and magnetic field strength- 860KA/m). The result shows that the surface roughness value decreases from 328.42 nm to 42.93 nm.

Kang et al. (2012) designed and developed a newly built magnetic abrasive finishing (with double dipole tip set) for finishing of austenite 304 stainless steel tubes. The finishing is done by mixed type magnetic abrasive consists of (80% iron particles and 20% magnetic abrasive) along with a soluble type barrel finishing compound. The process parameters were (magnetic flux- 1.26-1.29T, speed- 500-30000 rpm, processing time- 10 to 20 min and workpiece pole tip clearance- 0.3 mm). The initial surface roughness of 304 stainless steel

was 2-3 µm. The results obtained at 10000 rpm the surface roughness decrease from 2-3 µm to 0.1 µm (for 10 min) whereas, the surface roughness at 10000 rpm decrease from 2-3 µm to 0.11 µm (20 min).

Kordonski et al.(2004) performed their experiments on newly designed and developed magnetorheological jet finishing process for finishing of fused glass silica (optics). MR jet polishing system was mounted on 5-axis CNC stage equipped with polishing manage software developed with QED technology. The water and abrasives mixture are used for the preparation of MR fluid. The experimentation was also conducted on small concave fused glass silica with initial surface roughness were 210 nm p-v and 50 nm rms. The initial surface roughnesses of fused glass silica were 0.47 µm p-v, 0.14 µm rms. The roughness profile was measured with the help of (New View 500 white light) interferometer. The results concluded that the surface values of fused glass silica reduces to 13 nm p-v and 2 nm rms whereas, for concave fused glass silica reduces to 44 nm p-v and 6 nm rms.

Gheisari et al. (2014) developed a magnetorheological finishing process for ultra precision finishing of Aluminium work material (cylindrical type). The water based suspension of micron sized diamond particles are used for MR fluid. The optimum parameters were (current- 9A and working gap- 5 mm). The initial surface roughness of the work material was 170 nm. The experimentation was conducted in three stages. In first stage, the work material speed varies from 250-1000 rpm. In second stage, the process time varies from 20-100 min. In third stage, the effect of a fast RAM on the surface roughness was considered. The results concluded that the surface roughness value improves by 40 nm with the increase in rotational speed (1000 rpm). The surface roughness value decreases to 42 nm whereas through the raise in finishing time (90 min), the surface irregularity value improves by 78 nm when the fast RAM (with 0.5 m/sec) was applied.

2.2 Research gap

From the literature review, it has been observed that there is no present magnetorheological finishing (MRF) process which can finish external cylindrical surfaces such as groove, taper, step surfaces and threads. To overcome these challenges to finish the above surfaces, a turning type magnetorheological finishing process need to be developed which finish the surfaces similar as machining the surfaces by the turning operation. Magnetorheological polishing (MRP) fluid can be used for finishing medium at turning tool tip surface for

finishing the external cylindrical surfaces as similar to machining done by turning tool. MRP fluid comprises of carbonyl iron particles and silicon carbide abrasives scatter in the visco plastic medium of grease and heavy paraffin liquid. When magnetic field is applied the rheological property of the MRP fluid changes (Singh et. al 2011).

The main advantages of using the proposed turning type magnetorheological finishing process are as given below.

- It can finish both ferromagnetic and non ferromagnetic material.
- There is no wear of finishing medium as MRP fluid is continuously changes at the tool tip.
- Capable to achieve nano level of finishing as magnetorheological polishing fluid is used for finishing operation.
- It can finish cylindrical surfaces such as groove, taper, step surfaces and threads.

2.3 Objective of the present work

To achieve the main objective such as design and development of turning type magnetorheological finishing (MRF) process, the following sub-objectives are:-

- To study the distribution of magnetic flux density at the tool tip surface with workpiece using MAXWELL ANSOFT V13 software (student version).
- To CAD design and fabricate the turning type MRF tool.
- To design and fabricate the fixture to hold the MRF tool on the selected lathe machine.
- To demonstrate the process capability of developed turning type MRF process on external surfaces of cylindrical workpiece.

2.4 Methodology

The current work is to design and development of turning type Magnetorheological finishing process. The step by step methodology has been defining for the development of turning type MRF setup.

- Lathe machine specification.
- Finite element (FE) analysis of MRF tool using MAXWELL ANSOFT V13.
- CAD model of MRF tool.
- Design fixture for holding MRF tool.
- Mounting of MRF tool and fixture on lathe machine.

- The flow chart described in the figure 3.1 shows the design steps of followed in fabrication of the MRF tool.

The flow chart described in the Fig.1.16. shows the design steps followed in development of the MRF tool.

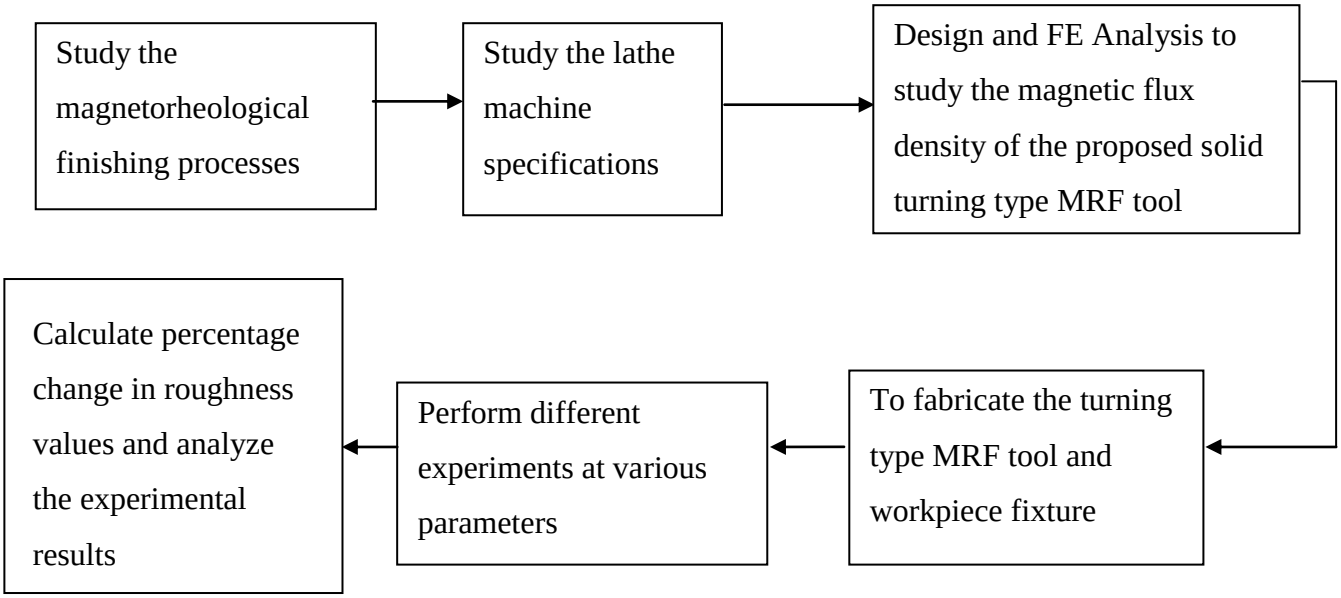

Figure 2.6: Flow diagram for the development of turning type MRF tool

Chapter-3

Design and Development of Turning Type Magnetorheological Finishing (MRF) Process

A novel precision finishing method used for cylindrical external surfaces with turning type magnetorheological finishing tool is developed. The method is used to finish the cylindrical external surfaces using magnetorheological polishing (MRP) fluid. This is a newly developed finishing process there is likely no existing MR finishing processes which can finish the external cylindrical external surfaces such as groove, taper, step surfaces and threads. A newly developed turning type magnetorheological finishing process is used for finishing external cylindrical surfaces, as tool tip is able to reach deeper grooves. This process can finish the work surfaces likely the same as the machining of cylindrical surfaces with CNC lathe cutter and release novel phase of their function in future. This turning type MRF method have its apparent functions in aerospace, automotive and machine tool industries**,** packing seal manufacturing industries, valve and pipe manufacturing industries.

3.1 Design and development of turning type magnetorheological finishing (MRF) process

The schematic representation of the turning type magnetorheological finishing process is shown in Fig 3.1.

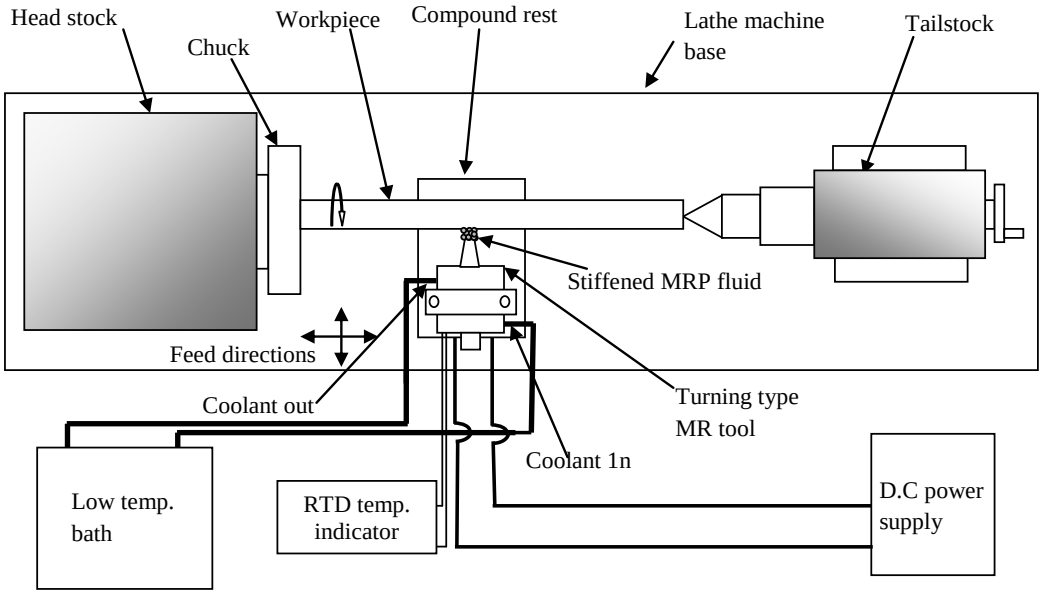

Figure 3.1: Schematic diagram of turning type MRF experimental setup

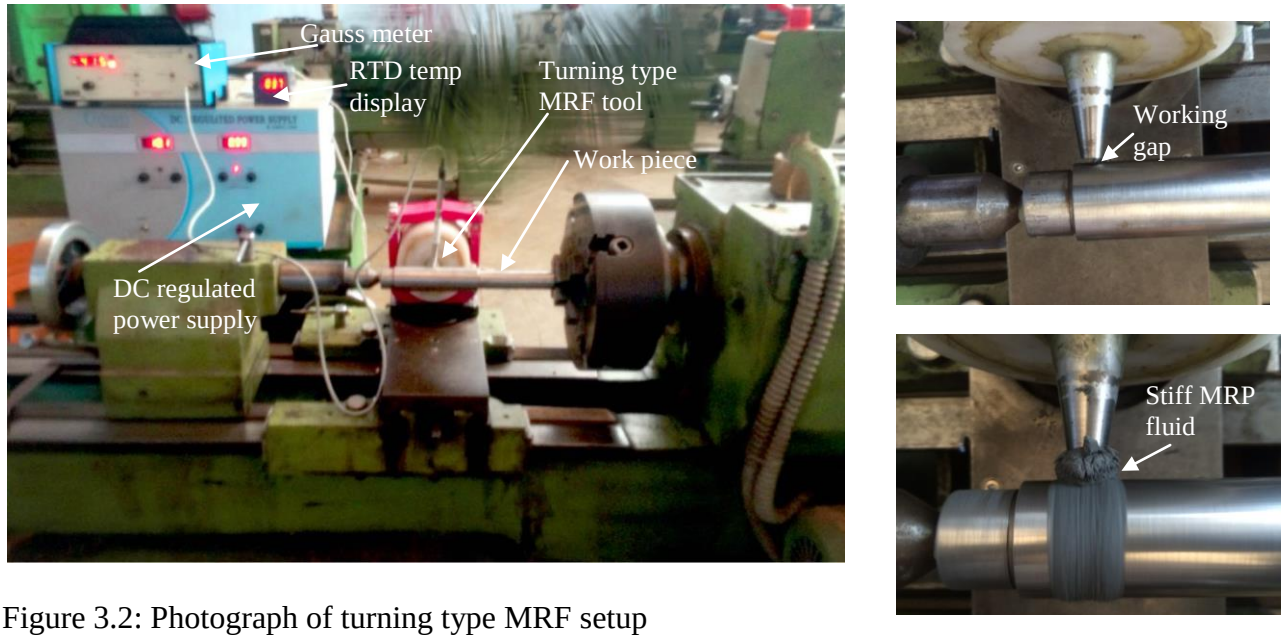

Figure 3.2: Photograph of turning type MRF setup

The magnetic field changes by varying the electric current that may change the viscosity of the magnetorheological polishing fluid (MRPF). As the magnetic field intensity is increased the viscosity of the fluid increase, the carbonyl iron particles (CIPs) attached towards tool tip and the abrasive are in between the CIPs chains and towards the workpiece for finishing (Singh et. al, 2011).

3.1.1 Mechanism of material removal

Material removal and surface finishing in turning type magnetorheological finishing process is based on abrasive action. When electromagnet is switched on, the MRP fluid is stiffed at the tool tip. When magnetic field is applied CIP particles holds abrasive grain give bonding strength to the MRP fluid. The nonmagnetic silicon carbide (Sic) abrasive particles that execute the cutting through machining are strongly bond in magnetic iron particles above the plane of thicken MRF tool. Due to relative motion between the work surface and tool tip for the duration of the rotation of work surface, the polishing mark created by MR particle chains through abrasive particles from the workpiece surface (Singh et. al, 2011). The mechanism of material removal in turning type magnetorheological finishing process is shown in Fig 3.3 above.

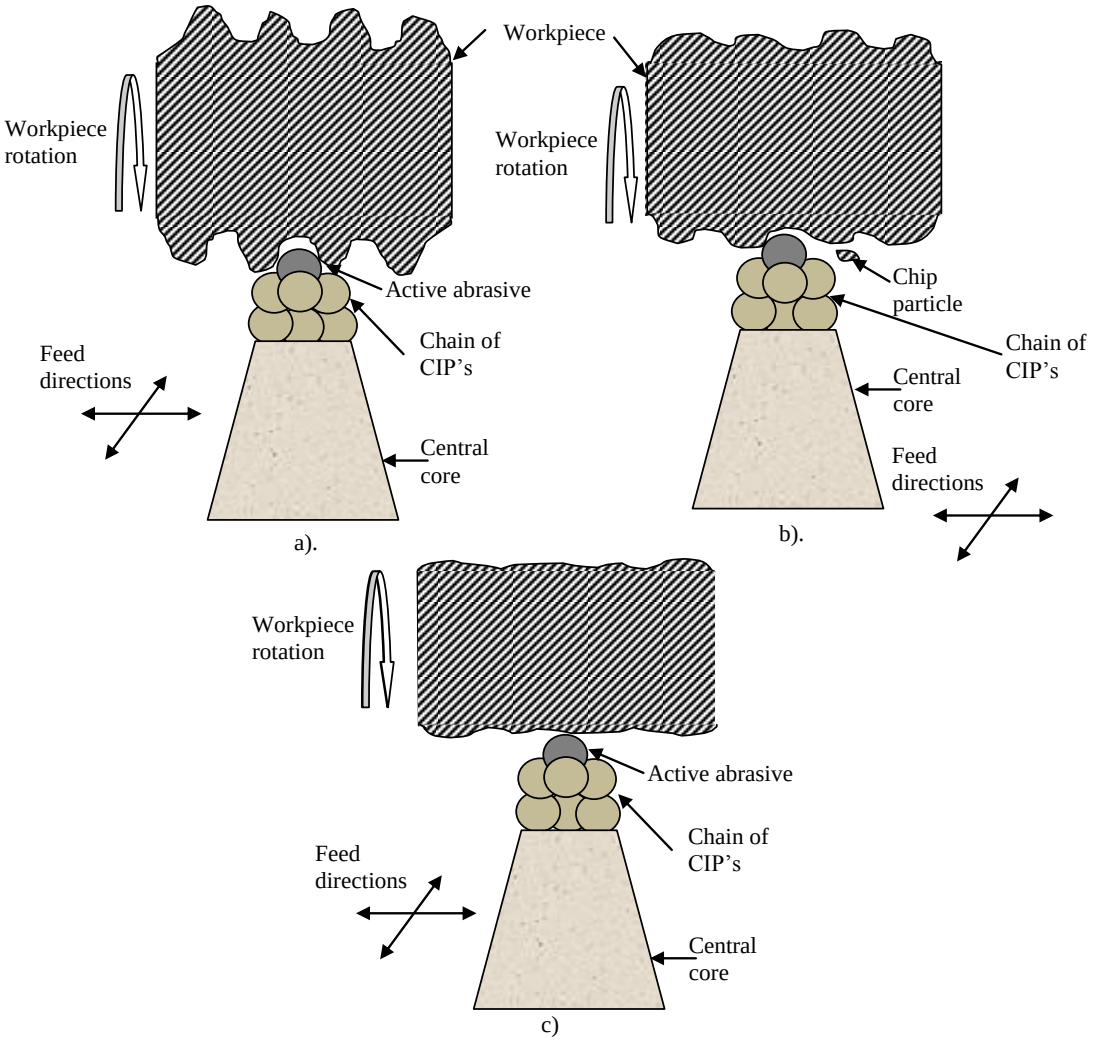

Figure 3.3: Schematic diagram of mechanism of material removal a) initial surface roughness peaks of workpiece and gripped CIPs with abrasive b). Chip removal in finishing c). Final roughness value after finishing

3.2 Finite element analysis of MRF tool

The Finite element analysis of MRF tool is done on MAXWELL ANSOFT V13 student version. The FE analysis helps in determining the value of magnetic flux density at various locations. There are different phases in MAXWELL ANSOFT V13 student version for FEM analysis. The phase used in this analysis is described below.

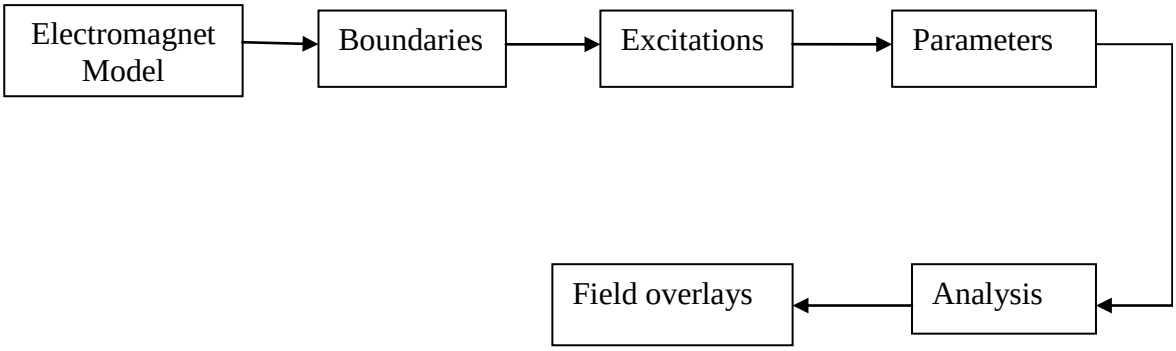

Figure 2.4: Flow chart of different phases in MAXWELL NASOFT V13

Starting from FEM analysis, initially draw electromagnet model in MAXWELL ANSOFT V13 student version. It is sub part of ANSYS which is used for magnetic field analysis. At the bottom of the electromagnet model dram a circle same as that of tool tip diameter and assign this permeability 5 that circle named as MRP fluid. Secondly, in FEM analysis boundaries constrain has selected in which different boundaries like insulating, master, slave etc. been chosen according to model setup. Here for MRF tool, coil has given an insulating boundary. As insulation is given coil appears with insulating hatching.

In the next step, in MAXWELL ANSOFT V13 excitations have selected. Further in excitations, there are different assigning parameters like current density, current, voltage density, voltage etc. In this, current which is in NI i.e. number of turns into current in ampere so according to number of turns current is selected and vice versa that is given at both the end of copper coil? Now in analysis, some parameters have selected to calculate the forces, torque etc. MAXWELL ANSOFT V13 having different parameters like torque, force and matrix. For MRF tool, we have to calculate force so parameter force is selected for calculating normal force at work piece in Newton.

For proceeding analysis add solution setup and assign a name then analyze the assigning name setup. In these step magnetic fields i.e. both B (tesla) field is drawn at proper plane to analysis magnetic field intensity.

For FE analysis, boundary conditions are working gap, electric current and number of turns on copper coil. But in this simulation both current and number of turns are varied to obtain different magnetic field intensity by which we keep current 3amp and number of turns 2200. The electromagnet model for MRF tool is shown in Fig 3.5.

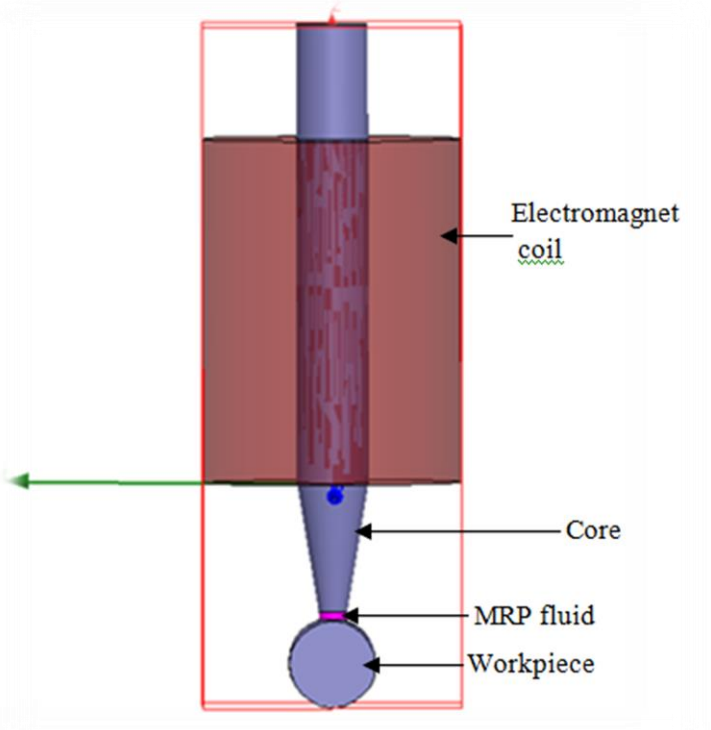

Figure 3.5: Electromagnet model of MRF tool

Parameters assigned to electromagnet model are shown in Table 3.1. The table shows assigned parameters, materials along and their relative permeability (it shows how dense the material is with respect to air). The number of copper wire turns in the coiling and current (in Amp.) supplied to this copper coil are also given in the table. All the simulation results are performed on the assigned data with varying working gap between the tool tip and the workpiece. The magnetic flux density distributions are also shown in simulation result.

Table 3.1: Parameters assigned to electromagnet model

Process Parameter	**Material**	**Relative permeability**	**Electromagnet Current**	**No. of turns**
Electromagnet coil	Copper	1	3A	2200
Inner core	Iron	1500		
MR polishing fluid	MRP fluid	5		
Ferromagnetic	Iron	1500		
Non ferromagnetic	Copper	1		

The simulation result for variation in magnetic flux density with ferromagnetic workpiece at different working gap is measured with the help of MAXWELL ANSOFT V13. The simulation result for the magnetic flux density for the 0.5mm working space among tool tip and the work surface. Variation for the magnetic flux density is shown in Fig 3.6. It is clear the magnetic flux density at the centre of the tool tip is near about 2 tesla when the working gap is 0.5mm that helps to hold the MRP fluid at the tool tip in such a way that the CIP chain particles are attached towards tool tip and abrasive are towards the workpiece That shows the maximum magnetic field intensity at the tool tip and it holds the magnetic and abrasive particles strongly (Singh et. al, 2011).

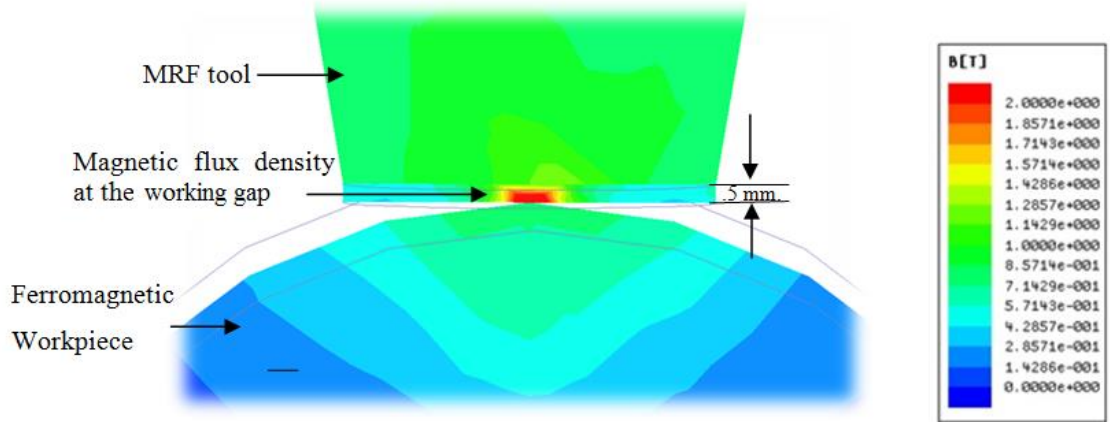

Figure 3.6: Magnetic flux density distribution (working gap=.5mm)

Simulation result shows as we move away from the central axis of the tool tip that shows uneven magnetic flux density distribution at the tool tip due to variation in working gap. As the workpiece is circular and tool tip is flat so that as we move away from the centre position the working gap varied that may affect the magnetic field density at the tool tip.

.

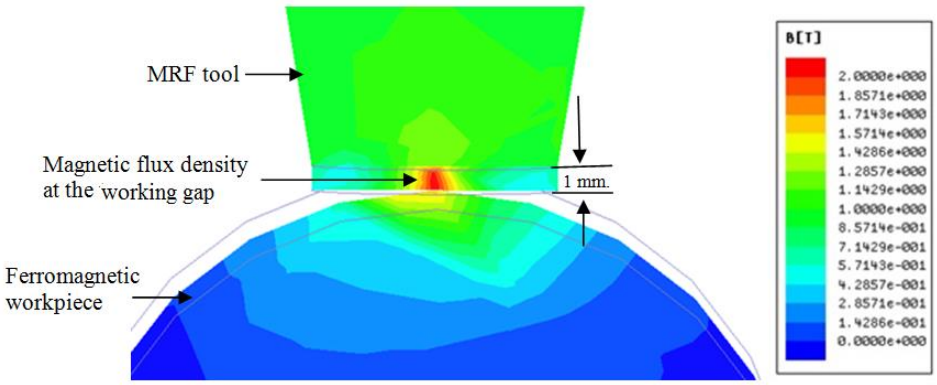

Figure 3.7: Magnetic flux density distribution (working gap=1mm)

Magnetic flux density at the centre of the tool surface is ~1.8571 tesla when the working gap is 1mm as shown in Fig 3.7. Magnetic line of forces are attract toward the workpiece as the

workpiece is of ferromagnetic material that helps to stiffened the MRP fluid at the tool tip to hold the abrasives in between the magnetized CIP particles.

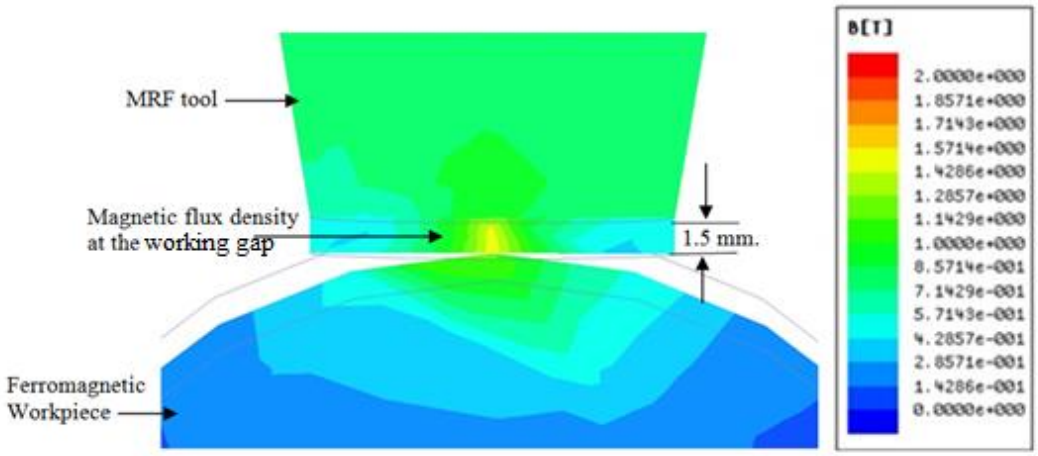

Figure 3.8: Magnetic flux density distribution (working gap=1.5mm)

Magnetic flux density at the centre of the tool surface is ~1.5714 tesla when the working gap is 1.5 mm as shown in Fig 3.8.

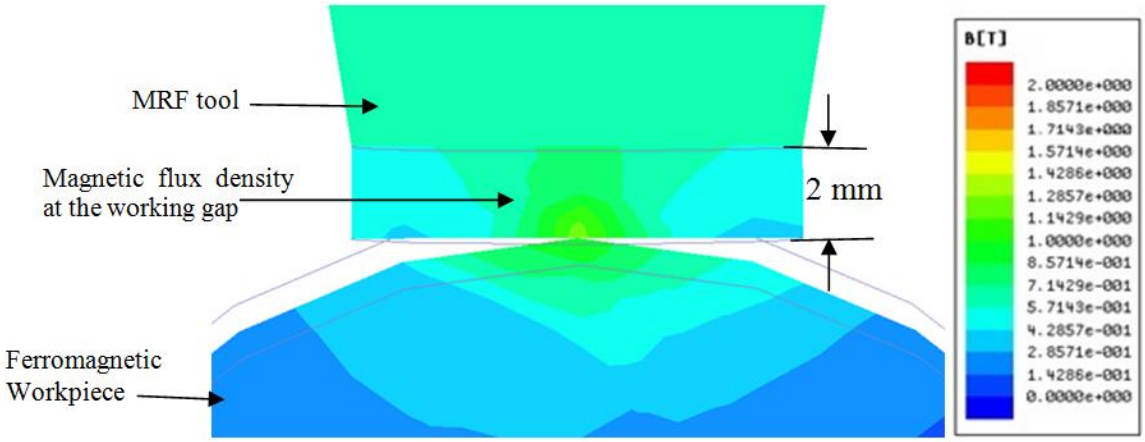

Figure 3.9: Magnetic flux density distribution (working gap=2 mm)

Magnetic flux density at the centre of the tool surface is ~1.3423 tesla when the working gap is 2.5 mm as shown in Fig 3.10.

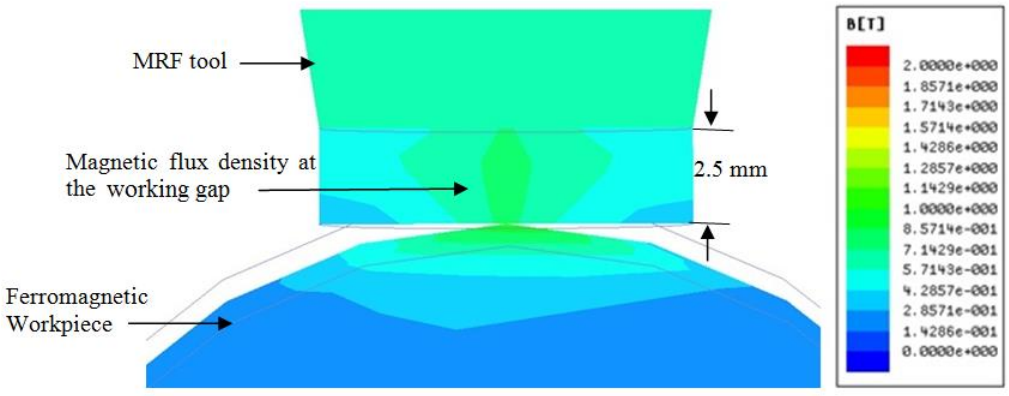

Figure 3.10: Magnetic flux density distribution (working gap=2.5 mm)

Magnetic flux density at the centre of the tool surface is ~1.4286 tesla when the working gap is 2.5 mm as shown in Fig 3.10.

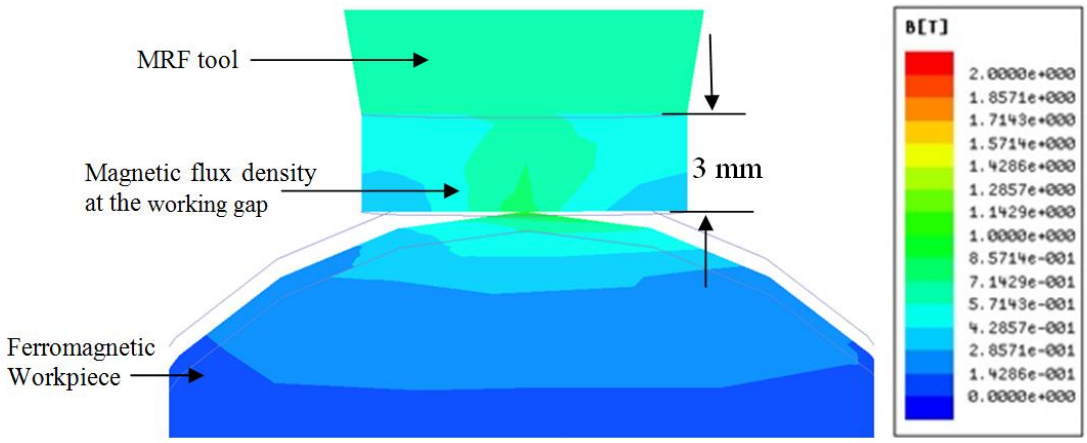

Figure 3.11: Magnetic flux density distribution (working gap=3 mm)

Magnetic flux density at the centre of the tool tip is ~1.3423 tesla when the working gap is 3 mm as shown in Fig 3.11.The magnetic field at the working gap 3 mm is less as we compare this with the working gap of 5 mm.

All the values from the simulation result with varying working gap is charted in the table 4.2 keeping electric current 3A number of turns in coiling 2200.With in MAXWELL ANSOFT V13 magnetic flux density as well as the normal force on workpiece is calculated. At the same working gap experimentally the magnetic flux density value is measured and charted as shown in table 3.2.

Table 3.2: Simulation and experimental result of turning type MRF tool

Sr. No.	**Process Parameters**			**Simulation results**		**Exp. result**
	Z(mm)	I(A)	M	Bz(T)	Fn(N)	Bz(T)
1	0.5	3	2200	2.0000	17.055	1.912
2	1.0			1.8571	15.792	1.789
3	1.5			1.5714	9.7116	1.598
4	2.0			1.4286	8.7854	1.472
5	2.5			1.3423	7.4535	1.385
6	3.0			1.2857	7.1958	1.240

Where Z = working gap in mm

I = current in ampere

M = number of turns

B_z = magnetic field in tesla

F_n = normal force on workpiece in Newton

Simulation and experimental results of magnetic field in tesla are plotted on graph at different working gap as shown in Fig 3.12. Experimental and simulation results are approximate equal that shows the minimum error in experimental and simulation results.

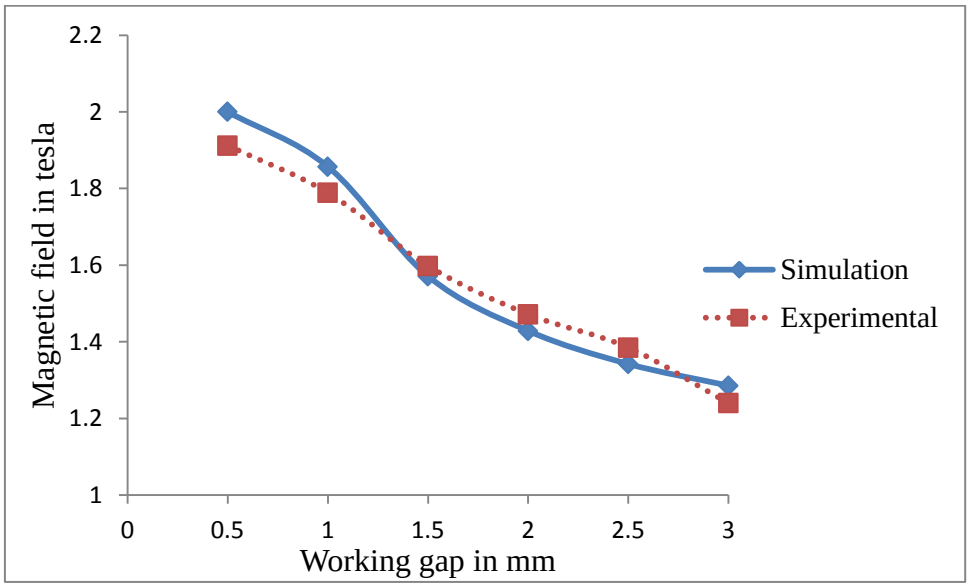

Figure 3.12: Graph between magnetic field v/s working gap

Figure 3.13 shows the variation of normal force on workpiece at different working gap. Graph shows as the working space among the tool as well as work surface increases the normal force on workpiece get reduced. Maximum force is induced at the working gap of .5 mm and it reduces further working gap increases.

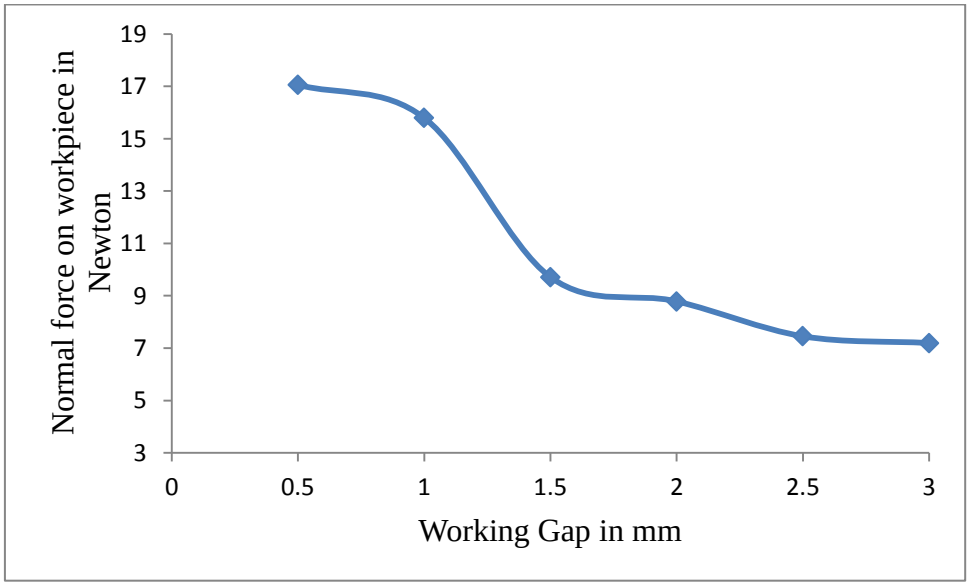

Figure 3.13 Graph between normal forces at work piece v/s working gap

It is observed from the simulation that the strength of the magnetic flux density is depends upon electric current and working gap. Strength of the MR fluid is control by controlling the electric current to the electromagnet coil. Experiments are conducted by varying electric

current from 1A to 5A.it is also observed that the working space among the tool as well as work surface is an important parameter for the strength of the finishing spot. It is observed that at the same electric current value by varying working gap the strength of the magnetic field changes. If working gap is minimum the MRP fluid become more stiffen as compare to more working gap at the same electric current. Experiments are conducted at the working range from 0 mm to 2.5 mm. From the Fig 3.12 and Fig 3.13 it is clear that normal force on workpiece and magnetic flux density are directly proportional to each other as the magnetic field increases the force value also get increased and vice versa. Using all this information obtains from the simulation result further design for the MR finishing tool is preceding.

3.3 Lathe machine specifications

Lathe is a machine tool which rotates the workpiece at its central axis to perform various operations the MRF tool which is applied to the workpiece is symmetric about the axis of rotation. The turning type MRF tool used to finish external cylindrical objects. The MRF tool is attached at the lathe machine for finishing the external cylindrical object. The lathe machine technical specifications are shown in table 3.3.

Table 3.3: Technical specification of lathe machine

Model	**1050/1**
Height of centers	175mm
swing over bed	335mm
Swing over saddle	230mm
Distance between centers	800mm
Bed	
Bed type	2 flat &2v
Bed width	254mm
Main spindle	
Spindle bore	42mm
Tail stock	
Spindle diameter	45mm
Tool slide	
Travel of tool slide	140mm
Speeds	
No. of speeds	8
Range RPM	45-938
Electrical	
Main motor	2HP/1440rpm
Other data	
Weight	800kgs
Floor space occupied (L*W)	1700*940

3.4 CAD model of turning type MRF tool

The whole turning type MRF tool comprises of sub parts which are given below

- Solid core
- Nylon bobbin
- Copper coiling
- Cooling jacket

The solid core is made up of mild steel material because it is having good magnetic properties. The stationary MRF tool is placed on X-Y slide. Two snap rings (circlips) are used to place nylon bobbin at proper position. The current is assigned to electromagnet model is 3A having 2200 number of turns. The material used for the coil is 20 gauge copper wire having relative permeability 1 and the material whose relative permeability is 1500 is used for the inner core. The relative permeability of the MRP fluid is assigned as 5. Transformer oil is used to cool the copper winding. The transformer oil is circulate with the help of low temperature bath and keeps in directly contact with copper winding that is inside the cooling jacket which is made of nylon material.

The CAD model of MRF tool and drawing of each part are shown in Fig. 3.14 and Fig. 3.15 respectively.

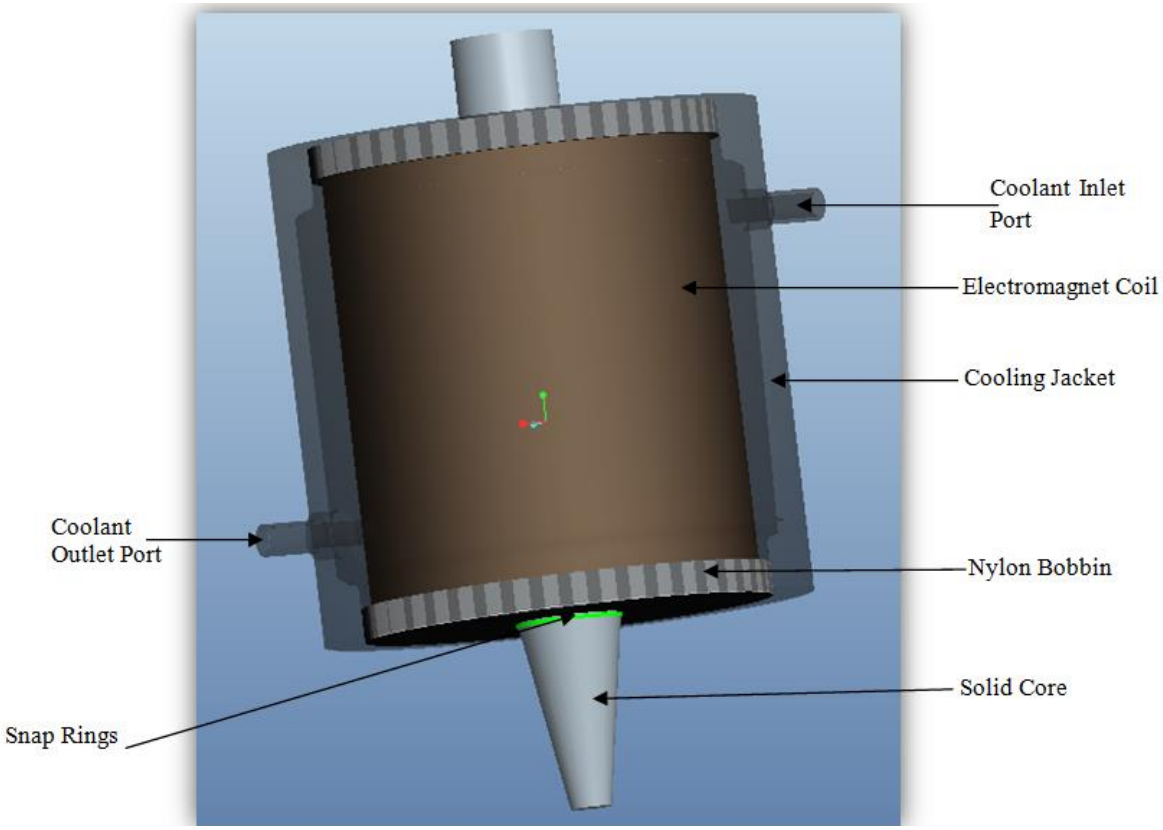

Figure 3.14: CAD model of MRF tool

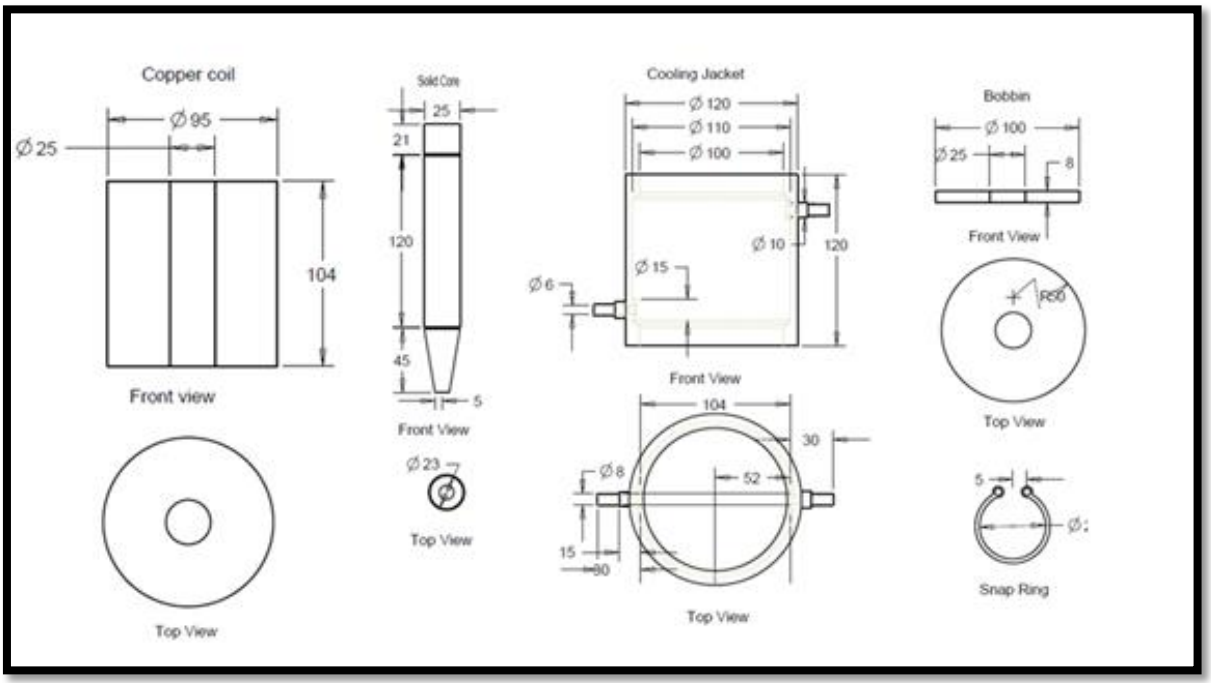

Figure 3.15: Drawings of MRF tool part

3.5 Fixtures for holding the MRF tool

The purpose of fixture is to locate and hold MRF tool. In the fixture of MRF tool which is shown below. The U shape clamp is used to hold the tool which is made up of aluminum because it is non-magnetic in nature and it will not disturb the induced magnetic field. The U shape clamp CAD model is shown below in Fig No. 3.16 the mechanical property of aluminum is shown in Table No. 3.4

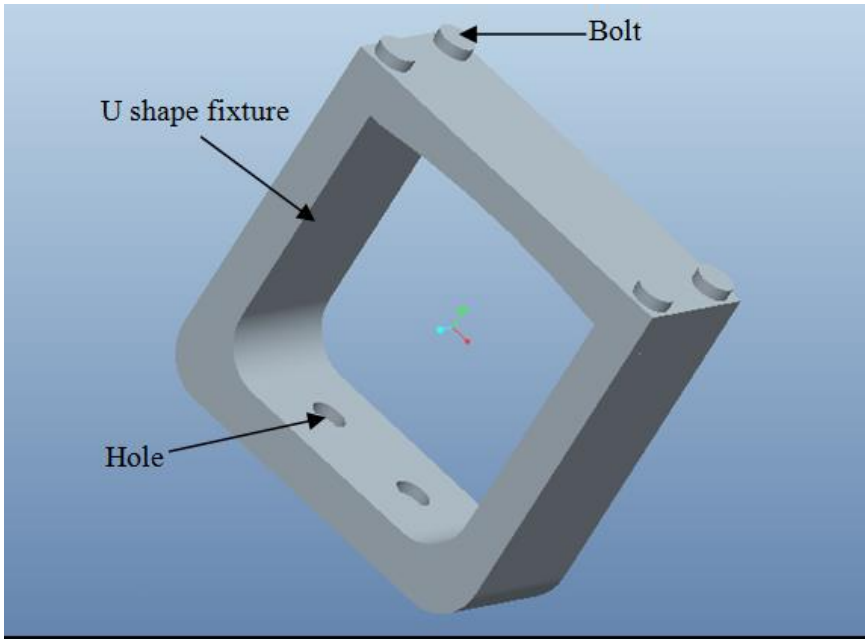

Figure 3.16: CAD model of MRF tool fixture

The following points should be keep in consideration while modeling a fixture are as follows

- Tool axis and workpiece axis are aligning to each other for proper finishing.
- The movement of X-Y slide should not block.
- U shape fixture is designed for proper holding.

Table 3.4: The mechanical properties of the aluminum 60610 for fixture (http://asm.matweb.com/search/SpecificMaterial.asp?bassnum=MA6061t6)

Density	2700 kg/m^3
Young's modulus	68.9 GPa
Ultimate tensile strength	124 MPa
Ultimate yield strength	55.2 MPa
Ultimate bearing strength	228 MPa
Poisson's ratio	0.33

The fixture helps in holding MRF tool. The cad model of whole MRF tool with all attachments is shown in Fig. 3.17 below-

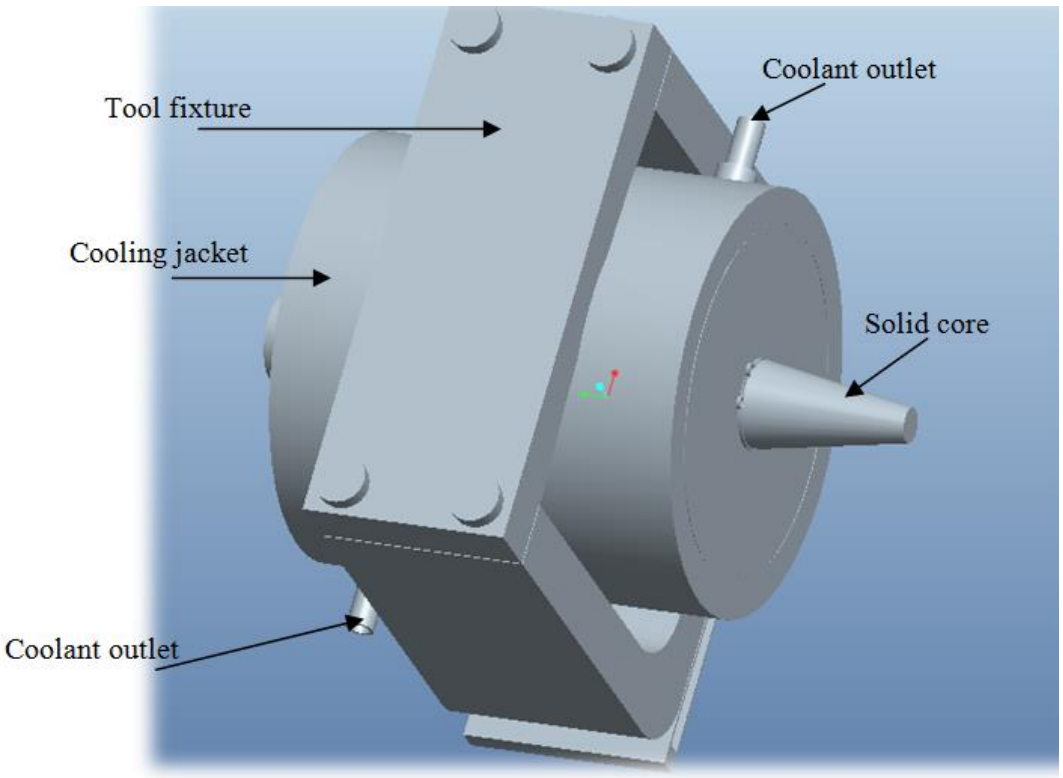

Figure 3.17: CAD model of MRF tool with fixture

Drawing of U shape clamp is shown in Fig 3.18 and 3.19.In Fig 3.18 fixture U shape as shown that holds the MRF tool and helps in to locate the tool on the lathe machine in such a way that the MRF tool which is applied to the workpiece is symmetric about the axis of rotation.

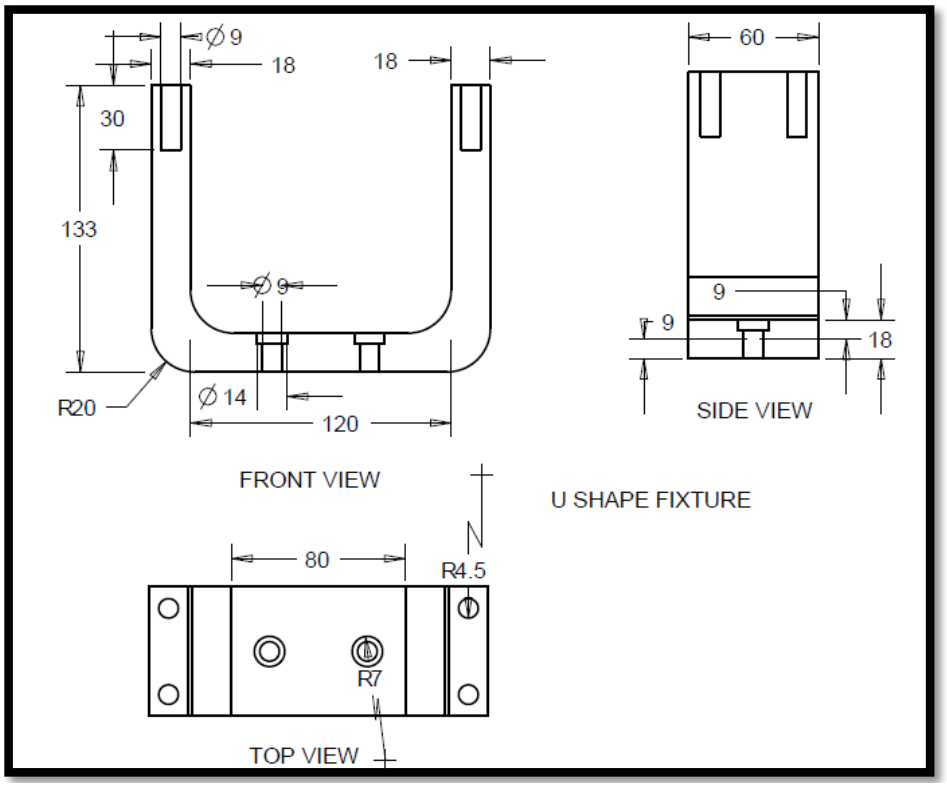

Figure 3.18: Drawing of u shape fixture

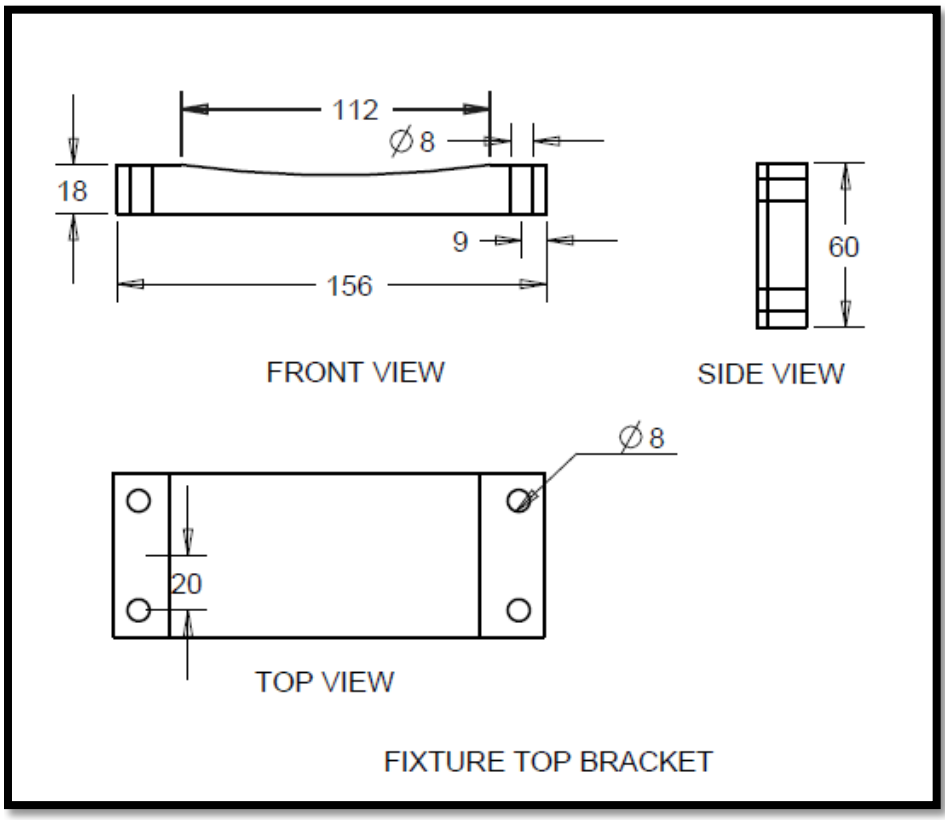

Figure 3.19: Drawing of fixture upper bracket

3.6 Mounting of MRF tool with fixture on lathe

Designed tool and fixture are mounted on compound rest .This MRF process is based on turning operation in which tool rotates and workpiece become stationary. The axis of workpiece and tool are align properly to maintain high level of finishing.tha assembled cad model of MRF tool and fixture on lathe machine as shown in Fig. 4.9.

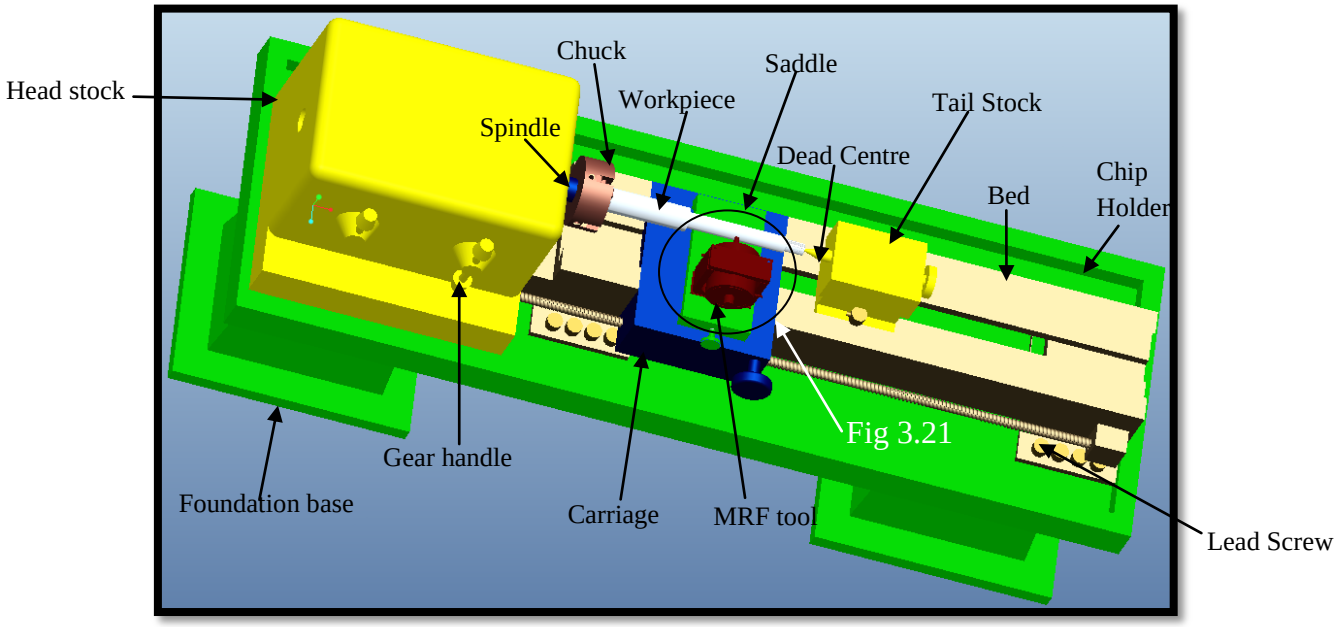

Figure: 3.20 CAD model of lathe with fixture

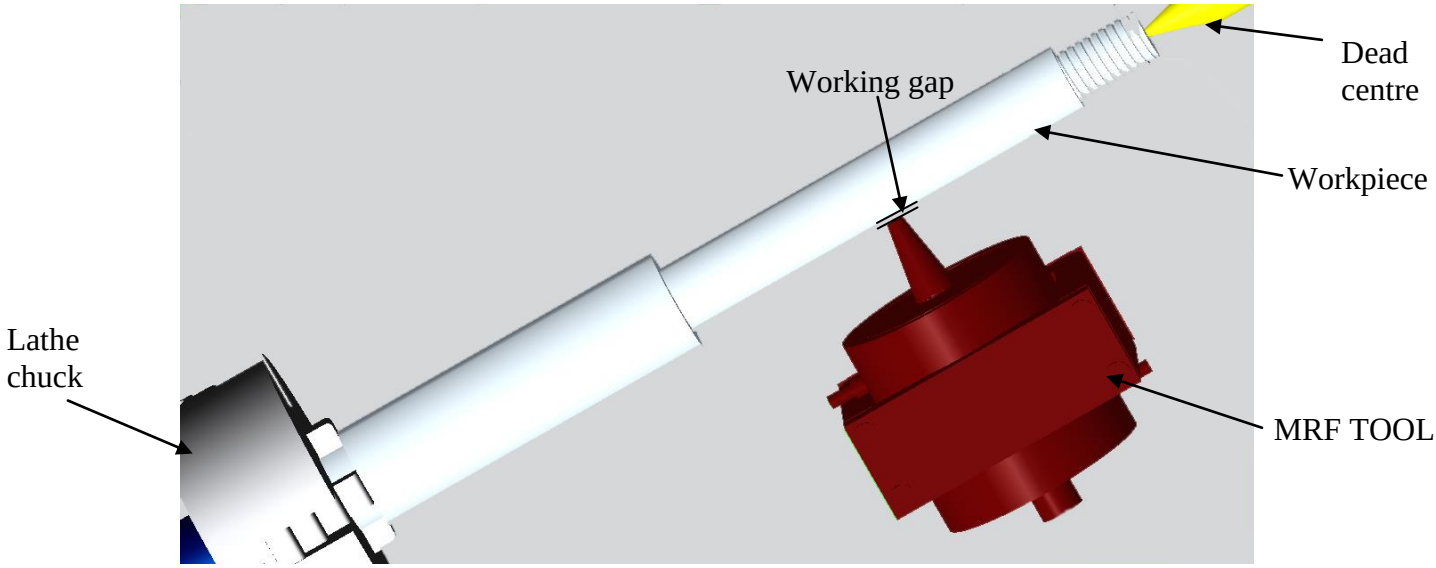

Figure 3.21: Zoom scale view of the MRF tool

1.1 CAD model of workpiece

The workpiece is made up of mild steel as it is ferro-magnetic in nature. The CAD model of the workpiece is shown in Fig 3.22. This ferro-magnetic workpiece finds its wide applications in macaroni manufacturing machine. The ultra fine surface finishing required at the outer surface of workpiece reducing the frictional and wearing losses.

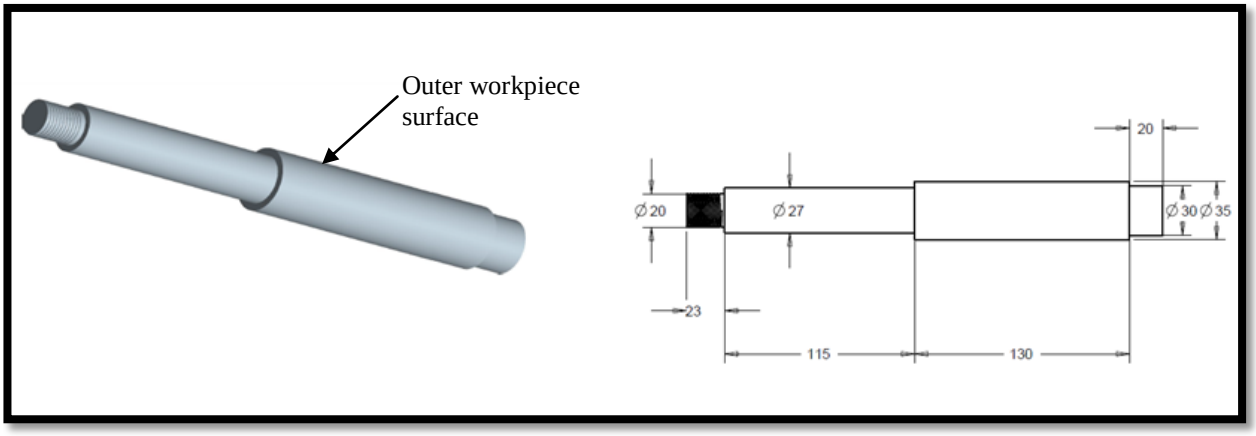

Figure 3.22: CAD model and drawing of workpiece

Chapter-4

Synthesis of MR Polishing Fluid and Experimentation

To study the performance of newly developed turning MRF tool, some preliminary experiments were performed on ferromagnetic work surface for studying the surface roughness.

4.1 Preparation of MRP fluid

MRP fluid is prepared with combination of 20 volume % of carbonyl iron particles, 20 volume % of abrasive particles (silicon carbide powder) and 60 volume % of base fluid (80 wt % of heavy paraffin oil and 20 wt% of AP3 grease) (Singh et.al).start with mixing the heavy paraffin oil and AP3 grease in stainless steel funnel with multi blade stirrer that is controlled by DC RPM controller on DC motor. Mix abrasives and carbonyl iron particles for some time and add into the base fluid. The mixing process is very slow process to avoid the sedimentation of carbonyl iron particles at the bottom of the mixing funnel.

4.1.1 Preparation of base fluid

In the composition of 1 kg (1000 grams) base fluid, heavy paraffin oil is 80% by weight= 800 gram And AP3 grease is 20% by weight= 200 gram.

Stirrer heavy paraffin oil for some time and include AP3 grease bit by bit into it. Keep stirring for sometime till both paraffin oil and grease mixed properly in each other. For density measurement take a sample of base fluid almost 20cm^3 and weight it.

Density = mass per unit volume.

Therefore, the density of base fluid=0.76 gm/cm^3

4.1.2 MR polishing fluid

Total quantity of MRP-fluid was prepared as 0.4 l=400 cm3.

Composition is CIP is 20% by volume =80 cm3 and by weight= 80 cm^3×7.8 gm/cm^3 (density of CIP) =624 gm/cm^3=0.624 kg. The silicon carbide abrasive powder is 20% by volume=80 cm^3 and by weight=80 cm^3×3.22 gm/cm^3 (density of silicon carbide abrasive powder) =257.6 gm. The base fluid is 60% by volume=400 cm3×60%=240 cm^3 and by weight=240 cm3×0.76 gm/cm^3 (density of base fluid) = 182.4 gm/cm^3.

The above mention MRP-fluid was stirred in funnel. The % volume concentration of Constituent to prepare MRP fluid is shown in table 4.1 below.

Table 4.1: Composition of MR polishing fluid

Component	**% Volume**
Base fluid medium	60
Silicon carbide of mesh size 800	20
Carbonyl iron powder of CS grade	20

4.1.3 Rheological characterization of synthesized MR polishing fluid

Using a equivalent plate type rheometer, the rheological characterization of the synthesized MR polishing (MRP) fluid was brought out in a shear mode. The shear rate was varied from 0 to 1000 s−1 and the magnetizing current in the range from 0 to 4 A. The gap was kept 1 mm between the parallel plates. During the experiments, the cooling temperature on the parallel plates was maintained at 25◦C. It is cleared from rheological characterization that when the magnetizing current increases from 0 to 4 A, viscosity increases and as the viscosity increases, the shear strength of the synthesized MR polishing fluid also increases.

Figure 4.1 show that when the magnetic flux density increases due to the increase in magnetizing current, the shear stress and the viscosity of the synthesized MRP fluid increase. This increment in viscosity helps in stiffness of MRP fluid on the tip of this present low cost ball end MR finishing process.

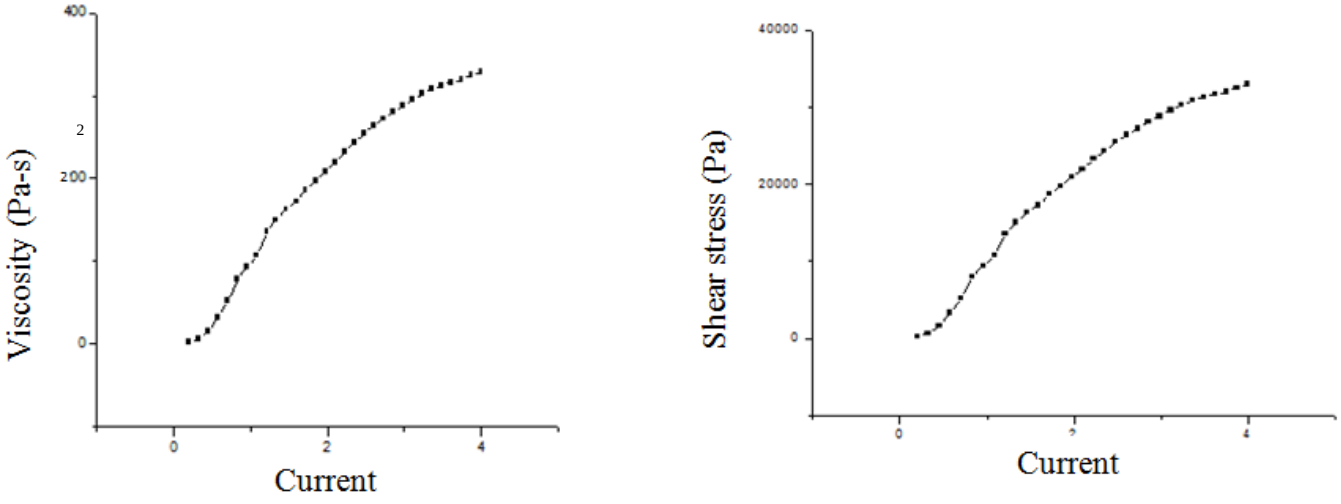

Figure 4.1: Graph between (a) viscosity and current (b) shear stress and current

4.2 Experimental study of magnetic field of MRF tool

To experimentally calculate the magnetic field at tip of MRF tool, the equipments used are given below-

- MRF tool
- DC power supply
- Gauss meter
- Real temperature display(RTD) temperature indicator

For magnetic field measurement joint positive and negative terminal of DC power supply with the terminals of electromagnet coil. DC power supply, is of 0-10 ampere current can be varying with the change in voltage from 0-100. During the coiling two PT-100 thermocouple are inserted between them to measure the coil inside temperature, that PT-100 are connect with RTD indicator is used for identifying temperature of thermocouple. For measuring the magnetic field gauss meter is used where 1 gauss = 0.0001 tesla. In probe type gauss meter magnetic field is measured by the probe that is having north and south poles at its tip. The gauss meter gives reading in gauss that is converted into the tesla (1 gauss= 0.0001 Tesla).

4.2.1 Experimental study of magnetic field of MRF tool without workpiece

The measurement of magnetic field at MRF tool tip without workpiece with graphs at different current is as follows.

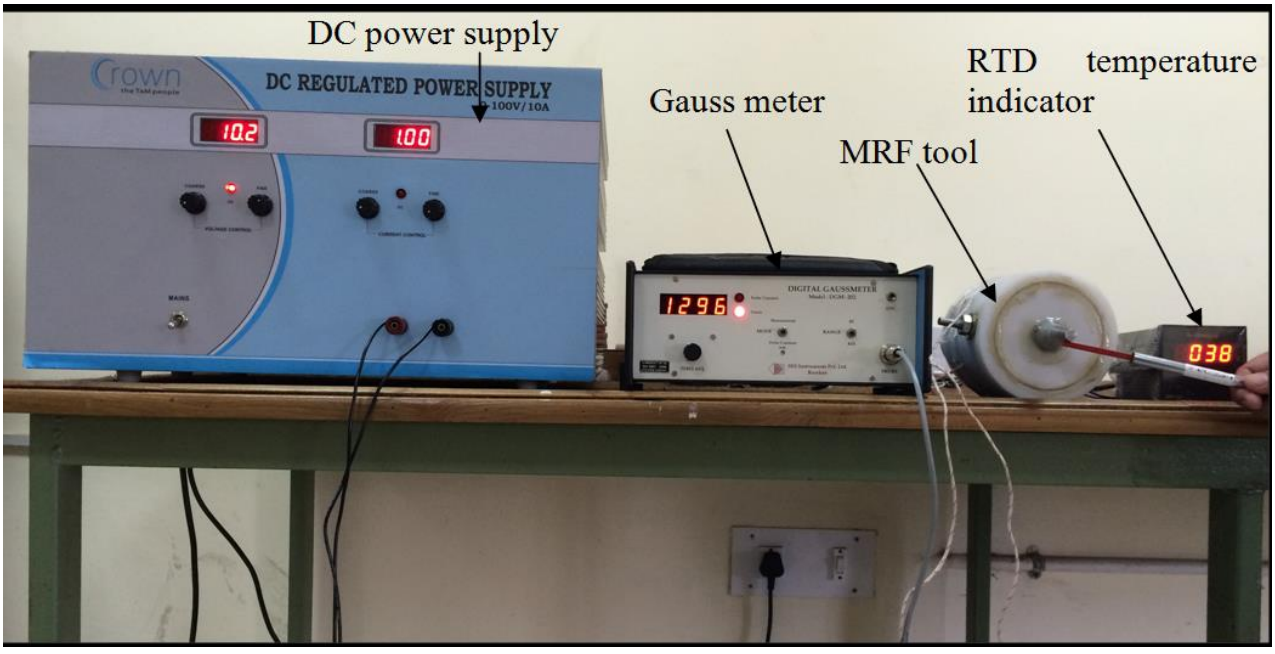

Figure 4.2: Experimental setup for measuring magnetic field without workpiece

Table 4.2: Experimentally study of magnetic field without workpiece

Distance in mm	Magnetic field in tesla		
	At 1 amp	At 2 amp	At 3 amp
1	0.170	0.231	0.231
2	0.213	0.332	0.325
3	0.551	0.741	0.745
4	0.655	0.836	0.825
5	0.751	0.884	0.878
6	0.762	0.873	0.865
7	0.675	0.828	0.842
8	0.563	0.743	0.755
9	0.245	0.345	0.345
10	0.190	0.220	0.225

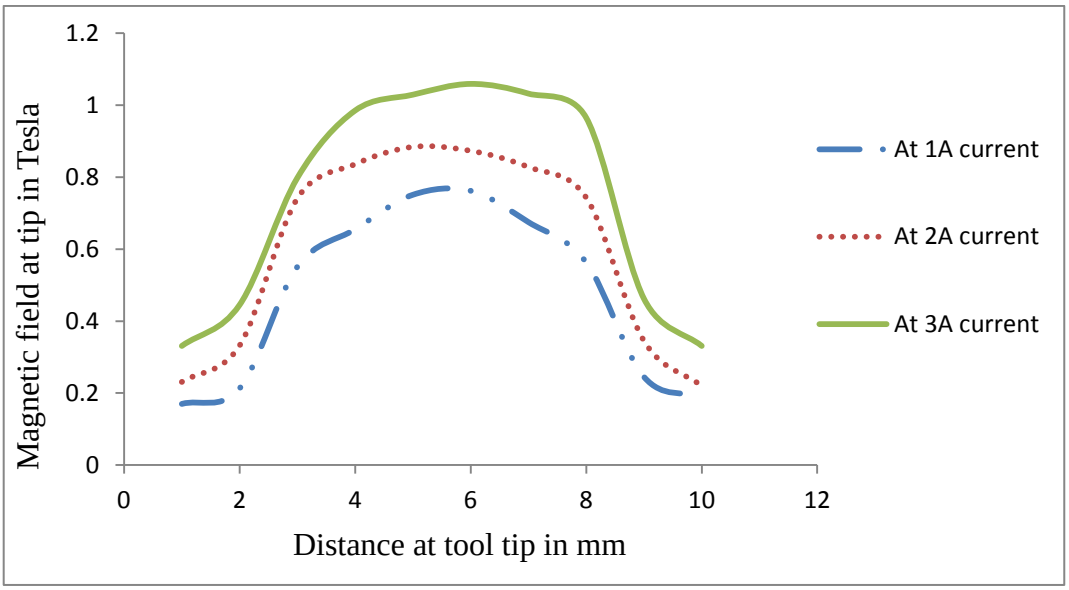

Figure 4.3: Graph between magnetic field and distance along core tip at different current

From the magnetic field measurement it is found that the change in electric current varies the magnetic field as shown in figure 4.3 as we increase the value of current the magnetic field is also increase. So the current affects the magnetic field during the finishing.

4.2.2 Magnetic field of MRF tool with workpiece

The magnetic field measurement with workpiece is measured experimentally at each 1mm distance at the tool tip. The gap between the tool tip and the workpiece is varied, at each gap the magnetic field is measured with the help of gauss meter that gives values in gauss further it is converted into Tesla (1 gauss = 0.001 Tesla). Experimental values and their graph are shown in below:

Table 4.3: Experimentally study of magnetic field with workpiece (current = 1A)

Distance at tool tip In mm	Magnetic field at tip in tesla					
	At 3mm gap	At 2.5mm gap	At 2mm gap	At 1.5mm gap	At 1mm gap	At 0.5mm gap
1	0.08	0.135	0.145	0.153	0.174	0.2
2	0.134	0.2	0.22	0.233	0.287	0.313
3	0.31	0.395	0.448	0.504	0.689	0.75
4	0.334	0.444	0.456	0.508	0.82	0.855
5	0.307	0.421	0.44	0.51	0.865	0.95
6	0.311	0.4	0.433	0.51	0.87	0.99
7	0.315	0.43	0.44	0.512	0.85	0.94
8	0.329	0.4	0.45	0.51	0.695	0.791
9	0.14	0.21	0.23	0.24	0.29	0.298
10	0.089	0.14	0.15	0.16	0.18	0.19

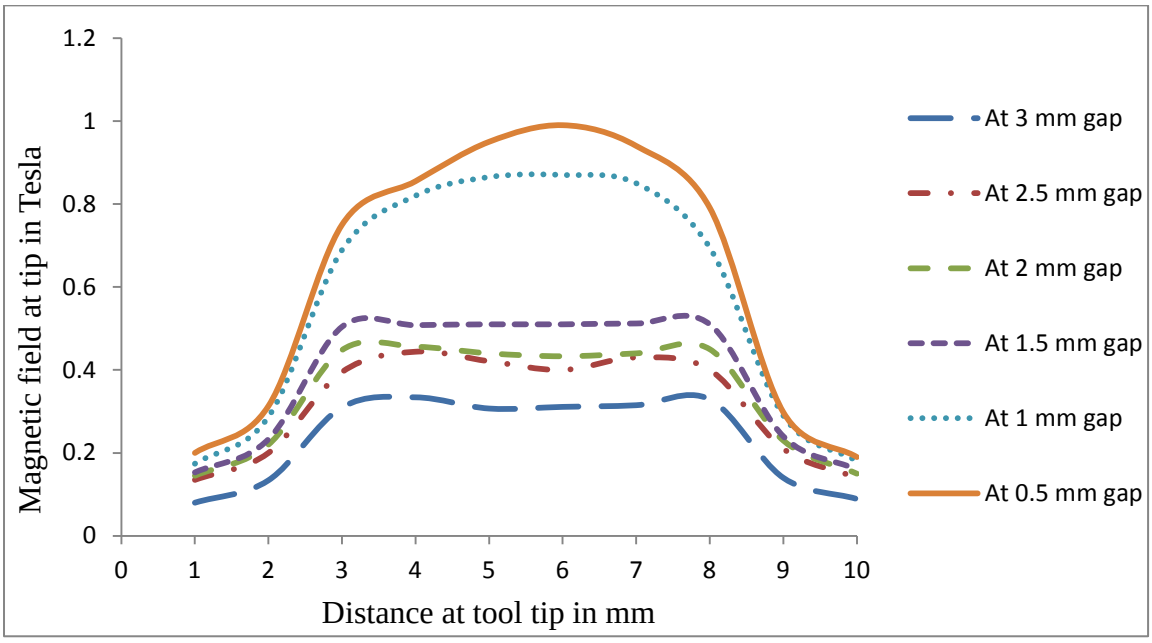

Figure 4.4: Graph between magnetic field and distance along core tip at different gaps with workpiece (current = 1A)

Table 4.3 shows the variation in the magnetic field at different working gap by keeping current at 1A.Figure 4.4 shows all the variation of magnetic field in graph, that clearly shows the magnetic field is maximum at the centre of the tool tip and almost symmetric at its central core axis. When working gap minimum then the magnetic field is maximum. At 3mm working gap the magnetic field is minimum and at 0.5mm working gap the magnetic field is maximum.

Table 4.4: Experimentally study of magnetic field with workpiece (current = 2A)

Distance at tool tip In mm	Magnetic field at tip in tesla					
	At 3mm gap	At 2.5mm gap	At 2mm gap	At 1.5mm gap	At 1mm gap	At 0.5mm gap
1	0.241	0.327	0.377	0.411	0.423	0.511
2	0.346	0.406	0.42	0.461	0.579	0.592
3	0.752	0.771	0.894	0.952	0.995	1.062
4	0.845	0.902	0.995	1.27	1.448	1.562
5	0.896	0.973	1.021	1.443	1.556	1.71
6	0.881	0.961	0.99	1.45	1.51	1.631
7	0.851	0.95	0.997	1.332	1.45	1.521
8	0.755	0.775	0.896	1.005	1.025	1.248
9	0.35	0.41	0.43	0.475	0.7	0.726
10	0.25	0.33	0.38	0.415	0.45	0.61

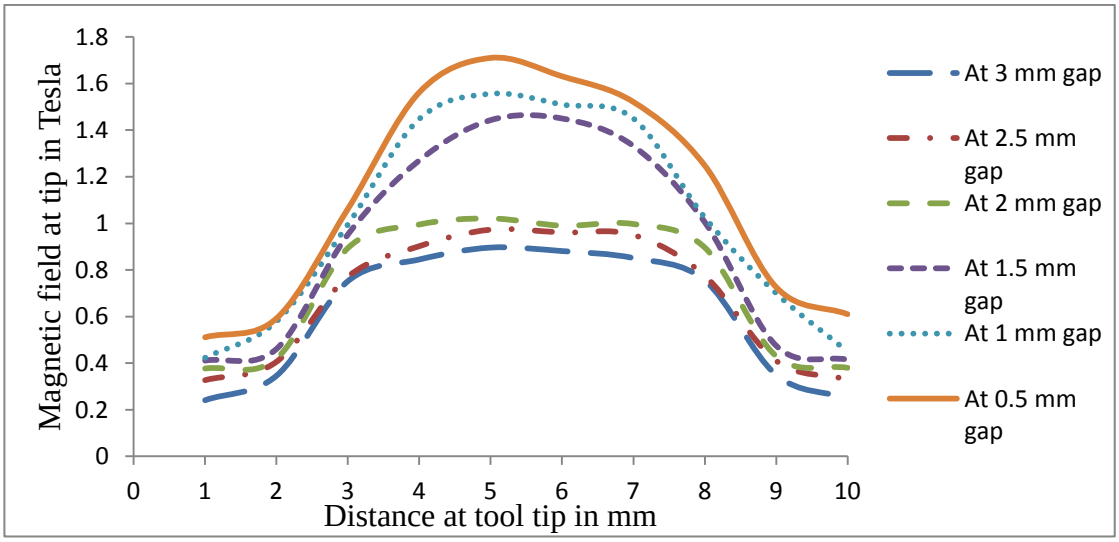

Figure 4.5: Graph between magnetic field and distance along core tip at different gaps with workpiece (current = 2A)

Table 4.5: Experimentally study of magnetic field with workpiece (current = 3A)

Distance at tool tip In mm	Magnetic field at tip in tesla					
	At 3mm gap	At 2.5mm gap	At 2mm gap	At 1.5mm gap	At 1mm gap	At 0.5mm gap
1	0.361	0.381	0.463	0.497	0.501	0.598
2	0.487	0.552	0.601	0.67	0.742	0.752
3	0.679	0.829	0.905	1.082	1.24	1.302
4	1.207	1.358	1.47	1.663	1.706	1.732
5	1.337	1.488	1.572	1.702	1.785	1.812
6	1.302	1.402	1.502	1.671	1.789	1.792
7	1.241	1.385	1.472	1.683	1.744	1.71
8	0.698	0.736	0.915	1.1	1.296	1.31
9	0.495	0.563	0.622	0.69	0.768	0.81

10	0.37	0.392	0.598	0.502	0.559	0.61

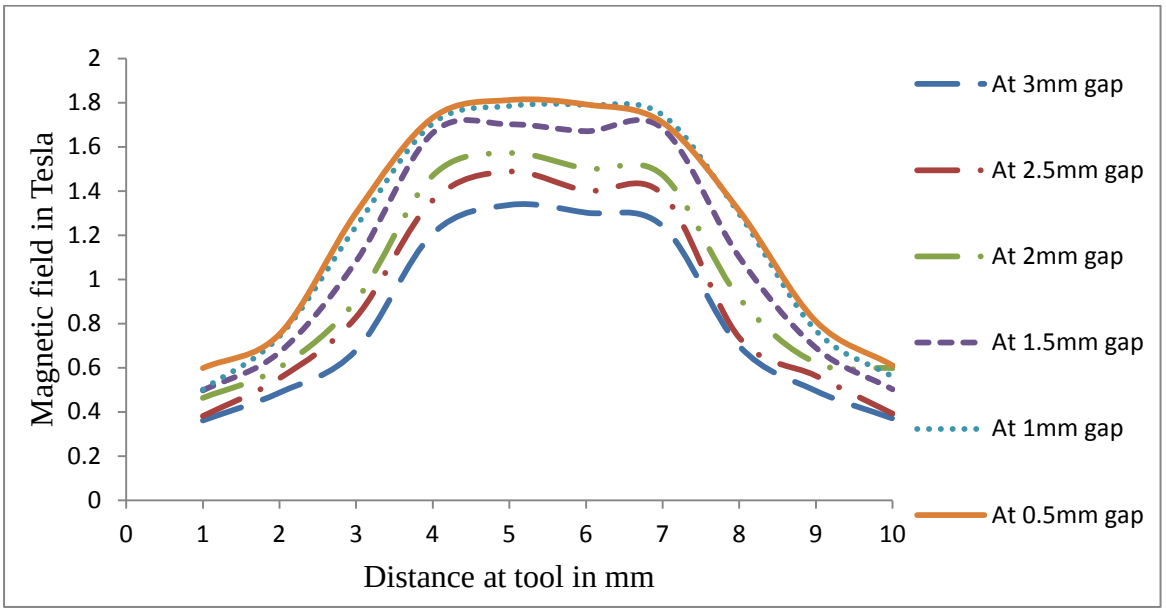

Figure 4.6: Graph between magnetic field and distance along core tip at different gaps with workpiece (current = 3A)

From the experimental results it has been noticed that the working gap is an important parameter which affects the magnetic field. At low working gap, the magnetic field is more as compared to higher working gap. The magnetic field at the centre of the tool tip is more due to the circular crossection of the workpiece whereas the shape of the tool tip is flat.

Statistical design of experiments (DOE) was used for the detail study for finishing of magnetic workpiece by the developed turning type magnetorheological finishing process. DOE is conduced to analysis the effect of workpiece rotation speed, working gap and the electric current on proportion change in surface roughness. Best finishing condition is obtained from these process parameters. It is observe that the proportion modify in R_a was most caused by working gap after that with magnetic current and the workpiece revolving speed. Scanning electron microscopy (SEM) was conducted to study the surface morphology.

4.3 Turning type MRF process variables

Turning type MRF process is a new finishing process for cylindrical external surfaces so be deficient in data is available in literature. Based on the other MRF process some controllable and uncontrollable process parameters are identified as shown in Table 4.6

4.3.1 Rotation speed of the workpiece (N)

Rotating speed of the workpiece effects the finishing of the work surface. The shear force is responsible for the material removal in form of micro chips during rotation of the work surface with the finishing spot of MRP fluid. Experiments are performed at speed 195 to 935 rpm; obtain from the level of arithmetic design. The series was selected on the basic of literature reviews.

Table 4.6: Turning type magnetorheological finishing process parameters

Independent controllable parameters	Dependent uncontrollable parameters
Rotational speed of workpiece	Ambient temperature
Working gap	Magnetic flux density
Magnetizing current	
Abrasive type, concentration and mesh size	
Carbonyl iron particle size and concentration	
Base medium volume percent and viscosity	

4.3.2 Electromagnet current (I)

The change in the rheological properties of turning type MRF process the finishing spot of the MRP- fluid at the tip mainly depends upon the magnetic flux density (supply of electric current in to the electromagnet coil). The finishing spot is also control by controlling the electric current. The bonding strength between the carbon iron particles is responsible for the material removal. The experiments are conducted from 0A to 4A. The values are selected as low first and then to high, as stated by the approved design of electromagnet.

4.3.3 Working gap (Z)

Working gap is space between the work surfaces along with the tip surface of the MRF tool. The finishing mark on the work surface is controlled by varying the working gap keeping the electric current to be constant. It means that, for the better finishing spot at the work surface and to remove max peaks, the tip of the tool keep closer to the work surface at constant current supply. Similarly when the tool tip is away from the work surface at the same magnetizing current the finishing spot of the MRP fluid is less stiff. The experiments are conducted in a working range of 0.5mm to 2.5mm. These values are chosen from the simulation result as presented in chapter-3.

4.4 Design of experiments

Planned experiments were used to explore the influence of variables on the percentage alteration in roughness value. The test performed on the turning type MRF process setup as shown in Fig 3.2 (chapter-3). Since the workpiece is in circular cross-sectional it is not easy to measure the surface morphology under a scanning electron microscopy (SEM), so to overcome this difficulties some small keys are cut in the workpiece of dimension 10*6*3 mm, which were option after grinding. The primary roughness was in series of 0.7 µm to 0.39 µm. the initial surface roughness is not alike for all the workpiece. The variation is taken by percentage modify in the surface roughness value specified by in Eq.4.1

The experimental setup is shown in Fig 3.2 in chapter 3. The workpiece is hold between the check and the dead centre on the Lathe machine for the rotation, MRF tool attached at the carriage for the X-Y movement of the slides. As the size of the tool tip thickness is 10mm and the workpiece size is same so that reciprocating motion in Y axis is not necessary during experimentation. The magnetizing current is switched on when MRP fluid is applied at the tool tip. A viscous structure of MRP- fluid created at the tip surface. In full factorial experiments, the combination of factors represents the each experimental condition, and their response is measured. To identify the significance of degeneration equation 'F' test via analysis of variance (ANOVA) was conducted. The percentage change in the roughness value is measured. The initially material removal from experiments was too low; hence it is not consider as much response.

Table 4.7 shows the actual as well as coded values in the turning type MRF process of ferromagnetic workpiece. Further experimental situation are scheduled in table 4.8. The turning type finishing process were performed on ferromagnetic workpiece the arbitrary experiments given in table 4.9

Table 4.7: Coded levels and equivalent actual values of the process parameters

S. No.	Parameter	Unit		Levels			
			-2	-1	0	1	2
1	Rotation speed of the workpiece(N)	RPM	195	288	384	598	938
2	Magnetizing current (I)	A	0	1	2	3	4
3	Working gap(Z)	mm	0.5	1	1.5	2	2.5

Note: - 195 rpm speed is not possible in selected lathe machine so the speed 195 rpm is taken as 145 rpm.

From the table 4.7 it is found that the speed of the workpiece varies from 195 rpm to 939 rpm, the electromagnet current is varied from 0A to 4A whereas the working gap is from 0.5mm to 2.5mm.

Table 4.8: experimental parameters and conditions

Parameters	Conditions
Finishing cycle time	90 min
Silicon carbide (SiC) abrasive powder (20 volume %)	800 mesh
Workpiece material	ferromagnetic

Table 4.9: Plan of experiments

Run order	Std. order	Actual values		
		N	I	Z
1	19	443	2	1.5
2	18	443	2	1.5
3	1	288	1	1
4	6	598	3	1
5	13	443	0	1.5
6	16	443	2	1.5
7	17	443	2	1.5
8	12	443	2	2.5
9	4	598	1	2
10	2	598	1	1
11	5	288	3	1
12	14	443	4	1.5
13	11	443	2	0.5
14	3	288	1	2
15	9	133	2	1.5
16	7	288	3	2
17	15	443	2	1.5
18	8	598	3	2
19	20	443	2	1.5
20	10	753	2	1.5

Table 4.10: Summary of response

Run	Factors			Initial average roughness value (µm)	Final average roughness value (µm)	% Change in roughness values
	N	I	Z	Ra_i	Ra_f	ΔRa(%)
1	443	2	1.5	0.56	0.4	28.6
2	443	2	1.5	0.67	0.48	28.35
3	288	1	1	0.54	0.40	25.93
4	598	3	1	0.60	0.37	38.33
5	443	0	1.5	0.5	0.5	0
6	443	2	1.5	0.51	0.35	31.37
7	443	2	1.5	0.64	0.43	32.81
8	443	2	2.5	0.59	0.56	5.1
9	598	1	2	0.54	0.49	9.26
10	598	1	1	0.52	0.40	23.07
11	288	3	1	0.58	0.34	41.37
12	443	4	1.5	0.65	0.46	29.23
13	443	2	0.5	0.68	0.31	54.41
14	288	1	2	0.5	0.45	10
15	133	2	1.5	0.63	0.46	26.98
16	288	3	2	0.68	0.51	25.00
17	443	2	1.5	0.52	0.35	32.69
18	598	3	2	0.58	0.48	17.24
19	443	2	1.5	0.62	0.41	33.87
20	753	2	1.5	0.52	0.41	21.15

4.5 Response surface regression analysis

The responses in provisions of initial roughness to final surface roughness (Ra) value and percentage alteration in roughness value (%ΔRa) are accessible in Table 4.9.

Percentage change in Ra value is calculated as.

$$\Delta Ra\ (\%) = [(Ra_i - Ra_f) / Ra_{i]} \times 100 \qquad (4.1)$$

To select the highest order polynomial the sequential model sum of squares was calculated. The model is not aliased due to some additional terms are significant. Table 4.10 shows of sequential model sum of squares show involvement of enhancing complication in overall model. Importance of count quadratic expressions to two factor interactions (2FI) and linear term is maximum, because it has smallest amount P- value and high F- value advising its suitability. Lack of fit for test is shown in table 4.11. For the chosen quadratic model, the lack of fit is insignificant.

On the foundation of Tables 4.10 and 4.11, quadratic model was chosen. During the initial experiments every term such as N, I, Z, NI, NZ, IZ, N^2, I^2 and Z^2 were integrated in the response surface model. The ANOVA for percentage modify in Ra is given in Table 4.12. The 67.88 *F*-value of model imply that the model is considerable. There is varying less (0.01%) probability that this great 'Model F-Value' could take place due to noise. For a significant model the 'Prob > F' value is less than 0.05.

In this case N, I, Z, $N^2$and I^2 is significant terms. If F-values is larger than 0.05 specify that terms are not considerable. By removing not important terms the model was enhanced. The 'lack of fit *F*-value' of 2.73 implies there is a 14.74% possibility that this large 'lack of fit *F*-value' could obtain because of noise.

Table 4.11: Sequential model sum of squares

Source	Sum of squares	DOF	Mean square	F-value	p- value Prob > F	Remarks
Mean versus total	13288.04	1	13288.04			
Linear versus mean	2552.24	3	850.75	22.02	<0.0001	
2FI versus linear	14.27	3	4.76	0.10	0.9572	
Quadratic versus 2FI*	499.47	3	166.49	15.94	0.0004	Suggested
Cubic versus quadratic	69.93	4	17.48	3.04	0.1085	Aliased
Residual	34.50	6	5.75			
Total	16458.46	20	822.92			

DOF: Degree of freedom, 2FI*: Two factors interaction

Table 4.12: Lack of fit tests

Source	Sum of squares	DOF	Mean square	F- value	p- value Prob > F	Remarks
Linear	590.15	11	53.65	9.58	0.0109	
2FI	575.89	8	71.99	12.85	0.0061	
Quadratic	76.42	5	15.28	2.73	0.1474	Suggested
Cubic	6.49	1	6.49	1.16	0.3311	Aliased
Pure error	28.01	5	5.60			

Table 4.13: ANOVA for percentage change in Ra

Source	Sum of squares	DOF	Mean square	F- value	p- value Prob > F	Remarks
Model	3065.98	9	340.66	32.62	<0.0001	Significant
N	43.73	1	43.73	4.19	0.0679	
Z	1716.24	1	1716.24	164.34	<0.0001	
I	792.28	1	792.28	75.87	<0.0001	
NZ	0.85	1	0.85	0.082	0.7811	
NI	6.18	1	6.18	0.59	0.4596	
ZI	7.24	1	7.24	0.69	0.4245	
N^2	97.21	1	97.21	9.31	0.0122	
Z^2	6.90	1	6.90	0.66	0.4353	
I^2	461.38	1	461.38	44.18	<0.0001	
Residual	104.43	1	10.44			
Lack of fit	76.42	10	15.28	2.73	0.1474	Not significant
Pure Error	28.01	5	5.60			
	3170.41	5				

Other ANOVA parameters are given in Table 4.14. The 'predicted R^2' value helps to determine how fine the model predicts a response value. The predicted R^2 and adjusted $R2$ should be within approximately 0.20 of each other. The predicted R^2 of 0.7892 is in reasonable closer to the familiar R^2 of 0.9374. 'Adequate Precision' (21.806) measures the

indication to noise ratio. A ratio greater than 4 is advantageous. In this model, this ratio of 21.806 shows an satisfactory signal.

Table 4.14: Other ANOVA parameters

Std. Dev. (SD)	3.23	*R2*	0.9671
Mean	25.78	Adj R^2	0.9374
C.V. %	12.54	Pred R^2	0.7892
PRESS *	668.37	Adeq Precision	21.806

S.D.: standard deviation, C.V.: Coefficient of variation, *Predicted residual sum of squares.

Table 4.15: Factor coefficients (coded form)

Factor	Coefficient estimate	DOF	Standard error	95% CI Low	95% CI High	VIF
Intercept	31.20	1	1.29	28.32	34.07	1.00
N	-1.65	1	0.81	-3.45	0.15	1.00
Z	-10.36	1	0.81	-12.16	-8.56	1.00
I	7.04	1	0.81	5.24	8.84	1.00
NZ	-0.33	1	1.14	-2.87	2.22	1.00
NI	-0.88	1	1.14	-3.42	1.67	1.00
ZI	-0.95	1	1.14	-3.50	1.59	1.00
N^2	-1.97	1	0.64	-3.40	-0.53	1.08
Z^2	-0.52	1	0.64	-1.96	0.91	1.08
I^2	-4.28	1	0.64	-5.72	-2.85	1.08

DOF: Degrees of freedom, CI: Confidence interval, VIF: Variance inflation factor.

For the coefficient estimate for the factor the 95% low and high confidence interval (CI) values are the lower and upper bound of the 95% confidence interval. These values in Table 4.15 represent the range that the true coefficient should be found in 95% of the time. If this range shows 0 (one limit is positive and the other negative) then the value of the coefficient of 0 could be true, indicating no effect of the factors. Lack of orthogonality in the design is measured by the variance inflation factor (VIF). If the value of VIF is one it shows factor is orthogonal to all other factors. If factors are too correlated together the value of VIF is greater than 10 Depending on the coefficients calculated in Table 4.15, the final equation is given as:

$\% \Delta Ra = 1.47861+0.079500\ N-8.75886\ Z+29.53715\ I-4.20968 \times 10^{-3}\ NZ-5.66935 \times 10^{-3}\ NI—1.90250\ ZI-8.18418 \times 10^{-5}\ N^2-2.09500\ Z^2-4.28375\ I^2$ (4.2)

For the model to be insignificant the p-value is greater than 0.05. There are

As *p*- value larger than 0.05 shows that the model expressions are not significant. There are four not important model conditions (Table 4.13), to improve the model dropping insignificant terms.

The ANOVA analysis after reducing the not important terms is accessible in Tables 4.16 and 4.17. The model F-value of 61.96 implies the model is considerable. Values of 'Prob > *F*' less than 0.05 indicates that the model conditions are considerable. Here *N*, *I*, *Z*, $N^2$and I^2 are significant model terms.

Table 4.16: ANOVA for % change in *Ra* after reducing the insignificant terms

Source	Sum of squares	DOF	Mean square	F- value	p- value Prob > F	Remarks
Model	3044.82	5	608.96	67.88	<0.0001	Significant
N	43.73	1	43.73	4.87	0.0445	
Z	1716.24	1	1716.24	191.30	<0.0001	
I	792.28	1	792.28	88.31	<0.0001	
N^2	90.59	1	90.59	10.10	0.0067	
I^2	458.58	1	458.58	51.12	0.0001	
Residual	125.60	14	8.97			
Lack of fit	97.58	9	10.84	1.94	0.2418	Non significant
Pure Error	28.01	5	5.60			

Table 4.17: other ANOVA parameters after model reduction

Std. Dev. (SD)	3.00	*R2*	0.9604
Mean	25.78	Adj R^2	0.9432
C.V. %	11.62	Pred R^2	0.9198
PRESS *	254.15	Adeq Precision	31.376

Factor reduction after model reduction as given in table 4.18 represents the range of true coefficient.

The final equation is:

$\% \Delta Ra = 20.48736+0.057708\ N-20.71375\ Z+23.72295\ I-7.71704 \times 10^{-5}\ N^2-4.17152\ I^2$ (4.3)

Table 4.18: Factor coefficients (coded form) after model reduction

Factor	Coefficient estimate	DOF	Standard error	95% CI Low	95% CI High	VIF
Intercept	31.60	1	0.98	28.49	32.70	1.00
N	-1.65	1	0.75	-3.26	-0.047	1.00
Z	-10.36	1	0.75	-11.96	-8.75	1.00
I	7.04	1	0.75	5.43	8.64	1.00
N^2	-1.87	1	0.58	-3.11	-0.60	1.03
I^2	-4.17	1	0.58	-5.42	-2.92	1.03

The percentage involvement of process parameter in ultimate retort of Ra as shown in table 4.19

Table 4.19: Percentage contribution of process parameter in final response of Ra

Source	Sum of squares	% contribution
N	43.73	1.40
Z	1716.24	54.84
I	792.28	25.31
N^2	90.59	2.90
I^2	458.58	14.65
Pure error	28.01	0.90

4.6 Result and discussion

Based on the results Eq.4.3 obtained after regression analysis, the results in terms of effect of magnetizing current, rotational speed of workpiece and working gap on the change in % ΔRa have been observed and computed. The effects of these variables in % change in *Ra* have been discussed as following.

4.6.1 Effect of rotation speed of workpiece

As seen in Fig 4.7 with increase in rotation speed of the workpiece the percentage change in surface roughness value reduces. At vary slow speed the percentage change in surface roughness value also reduces. This is because at higher rotational speed the MRP fluid

particles are disturbed, therefore magnetic normal forces magnetically decreases with increase in speed. As of result the CIP are not able to hold the abrasive particles strongly. Due to less magnetic normal force the active abrasives are scatter at the tool tip due to high speed. Since the centrifugal force (F_c) is proportional to square of speed.

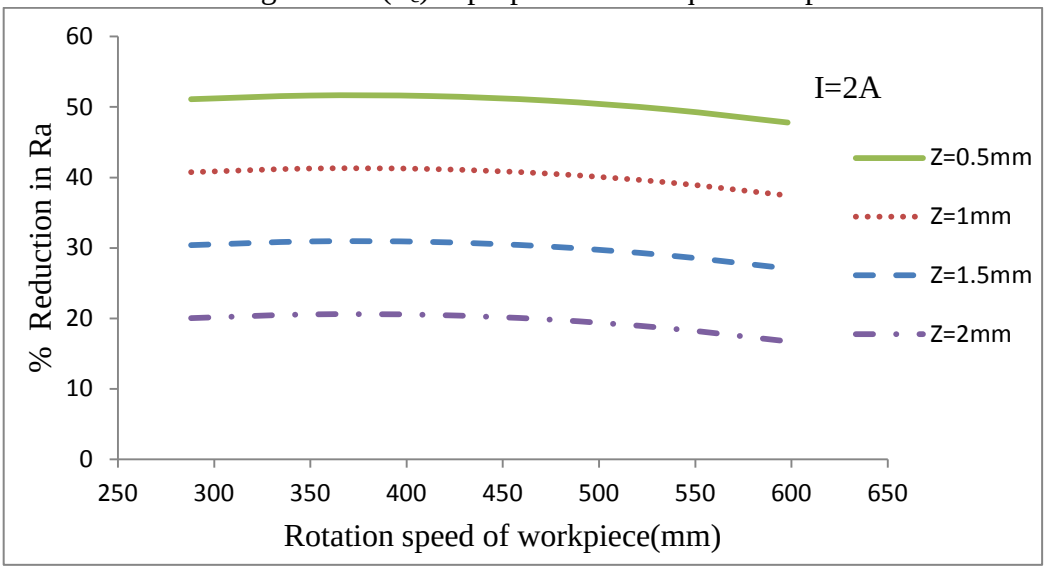

Figure 4.7: Effect of rotation speed on percentage reduction in Ra value

Therefore, with increase in percentage change in surface roughness value with increasing speed the F_c force plays an adverse role. Hence the magnetic normal force is higher than the centrifugal force (F_c) so that the CIP holds the abrasives strongly.

4.6.2 Effect of magnetizing current

The result of the magnetizing current on the proportion change in surface roughness value at varying working space and 443 rpm rotational workpiece speed is shown in Fig 4.8

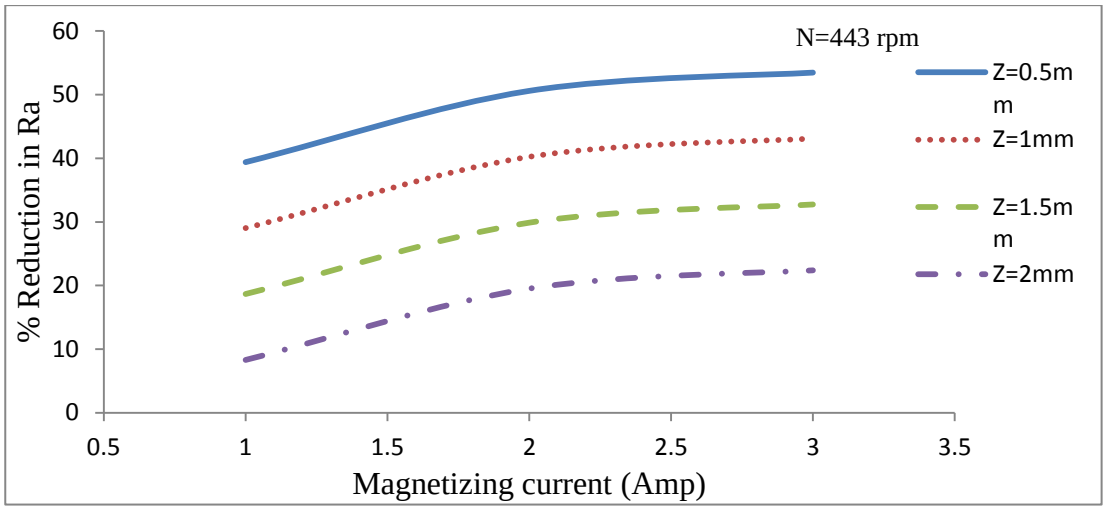

Figure 4.8: Effect of magnetizing current on proportion reduction in Ra value

by raise in magnetizing current the proportion vary in the surface roughness increases because by raise in the magnetizing current the magnetic flux density value increases as discusses in chapter -3 (table-3.2). Therefore, CIPs chains hold the abrasive strongly and result in increasing proportion vary in the surface roughness seen in Fig. 4.8.The contour and 3D plot for the result of rotational speed of the workpiece and working gap on the proportion vary in R_a as shown in Fig. 4.9

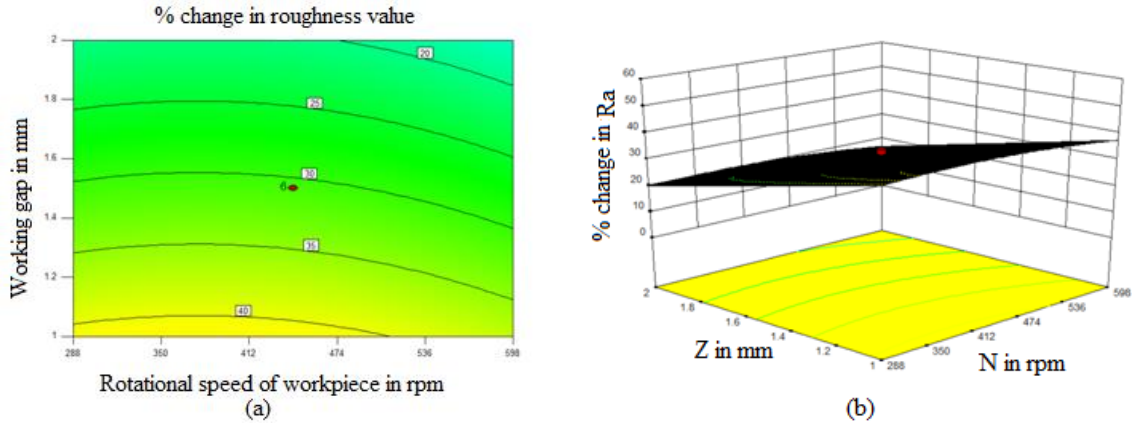

Figure 4.9 (a) Contour and (b) 3D plot of the variation of the %Ra value with electromagnet current and rotation speed of the tool.

4.6.3 Effect of working gap

The effect of % change in R_a value at varying magnetizing current and revolving speed of the workpiece is 443 rpm as shown in Fig. 4.10. It is observed that as the working space among the tool and the workpiece is increase the % change in R_a value decreases. Magnetic Flux density is impersonally proportional to the working gap. Therefore, when the working gap is minimizing the magnetic flux density is maximum at same current to the electromagnet coil and vice versa.

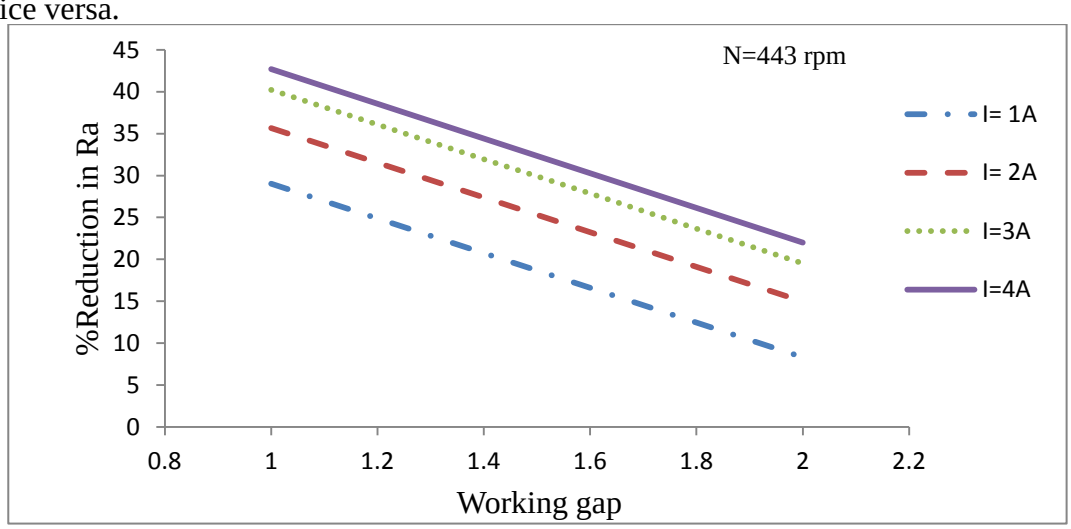

Figure 4.10: Effect of working gap on proportion reduction in Ra value

It is clear in the Fig 4.10 when working gap is reduced the percentage change in the roughness value is increased. As the working gap is less so the tool tip is much closer to the ferromagnetic workpiece, as the result the MR fluid strongly interacts with the workpiece. This may induce high magnetic normal force on the work surface. Equivalent shear strength get increased that may enlarge the percentage reduction in R_a value. Because the working gap greater than before at the same current the strength of the finishing mark got decreased, that may result to decrease the magnetic line of forces on the work surface. Because at the lower magnetic flux density the CIPs particles are not capable to holds the abrasives powerfully. Corresponding results to decrease in shear strength that may further reduce the % vary in the surface roughness value.

The most excellent finishing condition is best captured from the experimental data range of the variables is N=443 rpm, I=2A and Z=0.5mm. The surface roughness obtain after finishing at these conditions is 310 nm. The initial and final roughness profiles are shown in Fig 4.11(a) and (b) respectively.

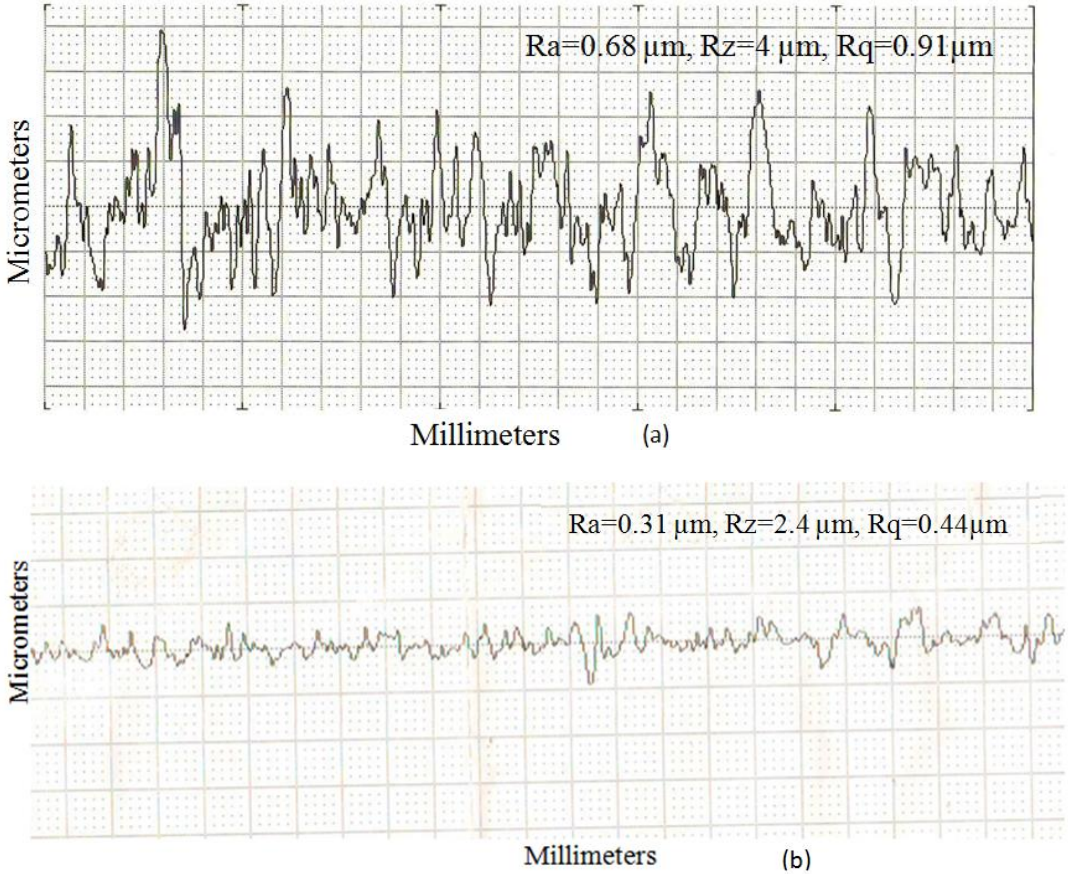

Figure 4.11: surface roughness profile (a) before (b) after turning type MRF for rotation speed 443 rpm, current= 2A and working gap 0.5mm. (Exp. No. 13 in Table 4.10)

The interactions of the cutting edges are not understood only by surface roughness profile. Therefore SEM was conducted for initial and final workpiece. The surface morphology of workpiece was observed at most excellent finishing situation with SEM at 1000x for primary and last roughness as sown in Fig 4.12 (a) and (b) respectively. Significant improvement is measured as compare to initial and final roughness profile. The finishing conditions is at N=443 rpm, I=2A and Z=0.5mm. The surface finish after finishing is measured 310 nm.

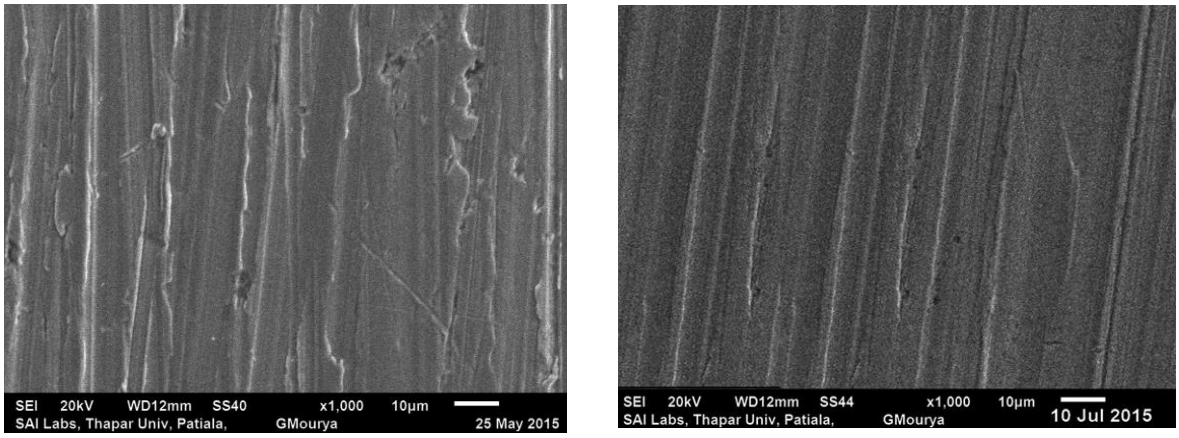

Figure 4.12: SEM micrograph at 1000x (a) before and (b) after turning type MRF for rotation speed 443 rpm, current= 2A and working gap 0.5mm. (Exp. No. 13 in Table 4.10)

4.6.4 Optimization of the developed process

As the maximum change in the surface roughness value is desired. So to achieve the maximum reduction in percentage value maximization of Eq. 4.3 is desired.

The optimum parameters are lies at rotation speed of workpiece is 195 rpm, magnetizing current 4A and 0.5mm working gap. The parameters are selected on basic of their effect in the %age change in the roughness value. The maximum % reduction is achieved at these values.

Chapter 5

Conclusions and Scope for Future Work

5.1 Conclusions

The turning type magnetorheological finishing process for finishing the external cylindrical work surfaces is designed and developed. Magnetic flux density distribution is analyzed at the tool tip using MAXWELL ANSOFT V13. CAD model was designed for the turning type magnetorheological finishing tool to examine the shape and dimensions. This turning type MRF process is a controllable process that is control by controlling the electric current that affects the final finishing surface. It has been seen that after experiments the parameters (electric current, speed of rotation and working gap) contributes in the finishing value. The following conclusions are made after experiments.

- It is found that the working gap is the largest part in affecting the percentage change in the roughness (R_a) value of the ferromagnetic workpiece.
- The best surface roughness value obtains ferromagnetic mild steel work piece was 310 nm from the initial roughness (R_a) value 680 nm at finishing condition of I = 2A, N = 443rpm working gap 0.5mm.
- The optimum surface reduction value obtains ferromagnetic mild steel work piece was 310 nm from the initial roughness (R_a) value 680 nm at finishing condition of I =2A ,N = 443rpm working gap 0.5mm.
- The ability of the turning type MRF process to reduce the surface roughness from 680 nm to 310 nm after 90 min of finishing and improve surface characteristic that shows the developed finishing method is able to finish cylindrical work surface.

The process is able to decrease the surface roughness and get better the surface characteristics of workpiece.

5.2 Scope for the future work

A problem must be solved for to allow the better nano level finishing with the help of this turning type magnetorheological finishing. The problem suggests a new research direction that is solved for better finishing in future.

As workpiece is of circular cross-section and turning type MRF tool tip is of flat surface so it is notice in the simulation the working space between the tool and the workpiece is varied as

we move away from the too tip, from the results it is found that the working gap is most influencing factor during the finishing. The result of that is uneven magnetic flux density on the tool tip.

The MRF tool CAD model with flat as well as circular cross- sections are as shown in Fig. 5.1 below:

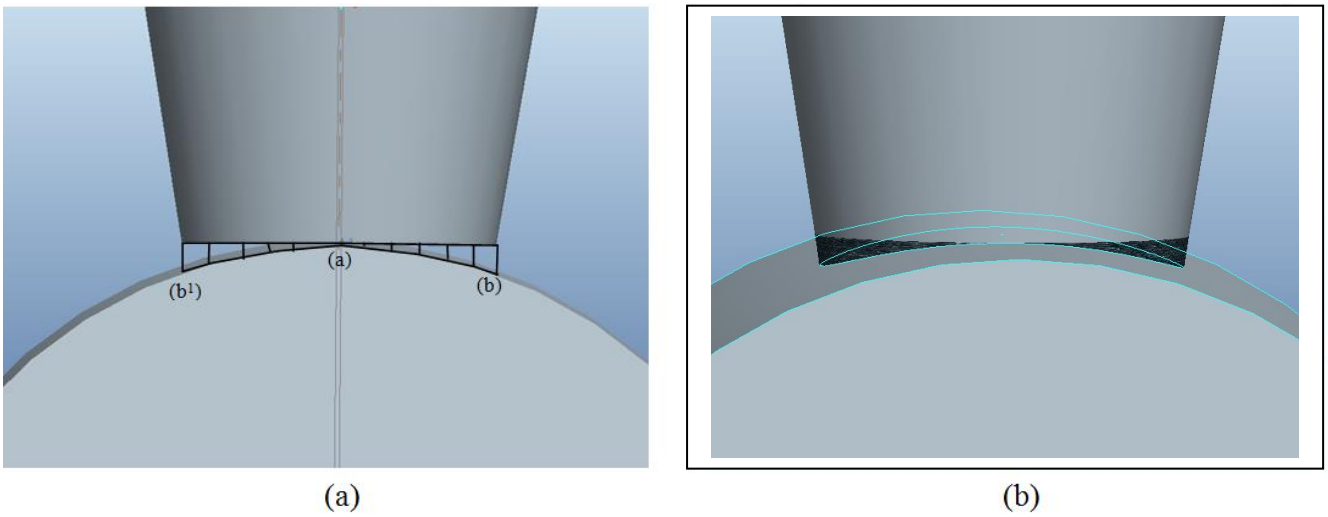

Figure 5.1(a) Present model (b) Future model of turning type MRF tool

Figure 5.1 (a) shows the difference of working gap between the tool and the work surface as we shift from position a to b or b^1. Figure also shows that the tool and work surface have point contact at point (a) and having some gap at point (b) depends upon the curvature of workpiece. This variation in the working gap disturbs the magnetic lines, so to design the tool tip as shown in Fig 5.1 (b) having surface contact between the tool and the work surface.

Lastly it is notifying that by maintaining the consistent working gap between the tool and work surface the level of finishing is improved.

A low temperature bath can be used for the effective finishing because at high current the temperature of the tool tip increases, that may results to decrease the viscosity of the MRP fluid. Due to decrease in the viscosity of the MRP fluid the carbon iron particles not able to hold the abrasives strongly so to maintain almost constant tool tip temperature low temperature bath can be used.

References

Cheng, H.; Yeung, Y.; Tong, H. (2008) Viscosity behaviour of magnetic suspensions in fluid-assisted finishing. *Progress in Natural Science*, 18: 91-96

Jain, V.K. (2008) Abrasive-based nano-finishing techniques. *Machining Science and Technology*, 12: 257-294.

Jain, V.K. (2009) Magnetic field assisted abrasive based micro-/nano-finishing. *Journal of Materials Processing Technology*, 209: 6022-6038.

Jha, S.; Jain, V.K. (2006) Modeling and simulation of surface roughness in magnetorheological abrasive flow finishing process. *Wear*, 261: 856-866.

Niranjan, M.; Jha, S.; Kotnala, R.K. (2014) Ball End magnetorheological finishing using bidisperse magnetorheological polishing fluid. *Materials and Manufacturing Processes*, 29: 487-492.

Shankar, R.M.; Jain, V.K.; Ramkumar, J. (2010) Rotational abrasive flow finishing process and its effects on finished surface topography. *International Journal of Machine Tools and Manufacture, 50: 637-650.*

Sidpara, A.; Jain, V.K. (2011) Experimental investigations into forces during magnetorheological fluid based finishing process. *International Journal of Machine Tools and Manufacture, 51: 358-362.*

Sidpara, A.; Jain, V.K. (2013) Analysis of forces on the free form surface in magnetorheological fluid based finishing process. *International Journal of Machine Tools and Manufacture*, 69: 1-10.

Singh, D.K.; Jain, V.K.; Raghuram, V. (2004) Parametric study of magnetic abrasive finishing process. *Journal of Materials Processing Technology*, 149: 22-29.

Sidpara, A.; Jain, V.K. (2012) Theoretical analysis of forces in magnetorheological fluid based finishing process. *International Journal of Material Sciences*, 56; 50-59.

Wang, A.C.; Lee, S.J. (2009) Study the characteristics of magnetic finishing with gel abrasive. International Journal of Machine Tools and Manufactures, 49; 1063-1069.

Singh, A.K.; Jha, S.; Pandey, P.M. (2012) Nano finishing of a typical 3D ferromagnetic workpiece using a ball end magnetorheological finishing process. *International Journal of Machine tools and Manufacture*, 63: 21-31.

Wang, Y.; & Hu, D. (2005) Study on the inner surface finishing of tubing by magnetic abrasive finishing. *International Journal of Machine Tools and Manufacture*, 45; 43-49.

Singh, A.K.; Jha, S.; Pandey, P.M. (2013) Mechanism of material removal in ball end magnetorheological finishing process. *Wear*, 302: 1180-1191.

Yamaguchi, H.; Shinmura, T. (2004) Internal finishing process for alumina ceramic components by a magnetic field assisted finishing process. *Precision Engineering*, 28: 135-142.

Cheng, H.; Feng, Y.; Wang, T.; Dong, Z. (2010) Magnetorheological finishing of optical surface combined with symmetrical tool function. *Frontiers of Optoelectronics*, 3(4): 408-412.

Cheng, H.; Feng, Y.; Wang, T.; Dong, Z. (2010) Magnetorheological finishing of optical surface combined with symmetrical tool function. *Frontiers of Optoelectronics*, 3(4): 408-412.

Das, M.; Jain, V.K.; Ghoshdastidar, P.S. (2008) Fluid flow analysis of magnetorheological abrasive flow finishing process. *International Journal of Machine Tools and Manufacture*, 48: 415-426.

Schmitt, C.; Moos, U.; Bahre, D. (2003) Comparison of different approaches to force controlled precision honing of bores. Journal of Mechanics Engineering and Automation, 3: 764-771.

Yin, S.; Shinmura, T. (2004) Vertical-assisted magnetic abrasive finishing and deburring for magnesium alloy. International Journal of Machine Tools and Manufacture, 44: 1297-1303

Gheisari, R.; Ghasemi, A.A.; Jafarkarimi, M.; Mohtaram, S. (2014) Experimental studies on the ultraprecision finishing of cylindrical surfaces using magnetorheological finishing process. Production & Manufacturing Research, 2:1: 550-557.

Kordonski, W.I.; Shorey, A.B.; Tricard, M. Nov (2004) Magnetorheological (MR) jet finishing technology. Proceeding of ASME International Mechanical Engineering Congress, 13-19: 1-8.

Judal, K.B.; Yadava, V.; Pathak, D. (2013) Experimental investigation of vibration assisted cylindrical magnet abrasive finishing of Aluminium workpiece. Materials and Manufacturing Processes, 28: 1196-1202.

Das, M.; Jain, V.K.; Ghoshdastidar, P.S. (2010) Nano Finishing of stainless steel using rotational magnetorheological abrasive flow finishing process. Machining Science and Technology, 14: 365-389.

Jha, S.; Jain, V.K.; Komanduri, R. (2007) Effect of extrusion pressure and number finishing cycles on the surface roughness in Magnetorheological abrasive flow finishing process.

International Journal of Advanced Manufacturing Technology, 33: 725-729.

Das, M.; Jain, V.K.; Ghoshdastidar, P.S. (2012) Nano finishing of flat workpiece using rotational magnetorheological abrasive flow finishing process. International Journal of Advanced Manufacturing Technology, 62: 405-420.

Hong, K.P.; Cho, Y.K.; Shin, B.C.; Cho, M.W.; Choi, S.B.; Cho, W.S.; Jae, J.J. (2012) MR fluid polishing of Alumina reinforced zirconia ceramics using diamond abrasive for dental application. Materials and Manufacturing Processes, 27: 1135-1138.

Kim, J.D. (1997) Development of a magnetic abrasive jet machining system for internal polishing of circular tubes. *Journal of Material Processing Technology* 71:384-393.

Seok, J., Lee, S.O., Jang, K.I., Min, B.K., Lee, S.J. (2009) Tribological properties of a magnetorheological (MR) fluid in a finishing process. *Tribology Transaction* 52(4):460-469.

Kordonski, W.I., Golini, D. (1999) Fundamentals of magnetorheological fluid utilization in high precision finishing, *Journal of Intelligent Material Systems and Structures* 10(9):683-689.

Jha, S., Jain, V.K. (2004) Design and development of the magnetorheological abrasive flow finishing (MRAFF) process, *International Journal of Machine Tools and Manufacture* 44, 1019-1029.

Kordonski, W. I., Shorey, A.B., Tricard, M. (2006) Magnetorheological jet finishing technology. *Transactions of ASME* 128:20-26.

Sidpara, A., Das, M., Jain, V.K. (2009) Rheological characterization of magnetorheological finishing fluid. *Materials and Manufacturing Processes* 24(2):1467-1478.

Bica, I. (2002) Damper with magnetorheological suspension. *Journal of Magnetism and Magnetic Materials* 241:196-200.

Genc, S., Phule, P.P. (2002) Rheological properties of magnetorheological fluids. *Smart Materials and Structures* 11:140-146.

Ruben, H.J. (1987) In: A. Niku-Lari (Ed.), Advances in Surface Treatments, Pergamon Press, Oxford: United Kingdom.

Furst, E.M., Gast, A.P. (2000) Micromechanics of magnetorheological suspensions. *Physics Revolution E* 61(6):6732-6739.

Brecker, J.N., Brown, R., Matsuo, T., Saito, K., Sweeney, J.A., Vansaun, J.B., Shaw, M.C. (1969) Abrasive Grain Association on Investigation of Abrasive Grain Characteristics, 4th Annual Report, Carnegie Institute of Technology, USA.

Bayoumi, M.R.; Abdellatif, A.K. (1995) Effect of surface finish on fatigue strength. Engineering Fracture Mechanics, 51(5): 861-70.

Zantye, P.B.; Kumar, A.; Sikder, A.K. (2004) Chemical mechanical planarization for micro-electronics applications. Material Science and Technology R, (45): 89-220.

Rhoades, L.J. (1988) Abrasive flow machining, Manufacturing Engineering, (1): 75-78.

Uhlmann, E.; Doits, M.; Schmiedel, C. (2013) Development of a material model for visco-elastic abrasive medium in Abrasive Flow Machining. Procedia CIRP, (8): 351-356.

Lam, S.Y. (2000) Process monitoring of abrasive flow machining using a neural network predictive model, Technical paper, University of Pittsburgh: Pittsburgh, PA.

Mori, Y., Yamauchi, K., Endo, K. (1987) Elastic Emission machining. *Precision Engineering* 9(3):123-128.

Jain, V.K. (2009) Magnetic field assisted abrasive based micro-/nano-finishing. *Journal of Materials Processing Technology* 209:6022-6038.

Kordonski, W.I., Golini, D. (1999) Fundamentals of magnetorheological fluid utilization in high precision finishing, *Journal of Intelligent Material Systems and Structures* 10(9):683-689.

Jha, S., Jain, V.K. (2004) Design and development of the magnetorheological abrasive flow finishing (MRAFF) process, *International Journal of Machine Tools and Manufacture* 44, 1019-1029.

Sadiq, A. Shunmugan, M.S. (2010) A novel method to improve finish on non-magnetic surface in magnetorheological abrasive honing process. *Tribology International 43:1122-1126.*

Sadiq, A., Shunmugan, M.S. (2009) Investigation into magnetorheological abrasive honing. International Journal of Machine Tools and Manufacture 49:554-560.

Singh, A.K.; Jha, S.; Pandey, P.M. (2011) Design and development of nanofinishing process for 3D surfaces using ball end MR finishing tool. *International Journal of Machine Tools and Manufacture*, 51:142-151.